Biomaterials Science

REVIEW

Cite this: *Biomater. Sci.*, 2017, **5**, 353

Recent applications of the combination of mesoporous silica nanoparticles with nucleic acids: development of bioresponsive devices, carriers and sensors

Rafael R. Castillo, Alejandro Baeza and María Vallet-Regí*

The discovery and control of the biological roles mediated by nucleic acids have turned them into a powerful tool for the development of advanced biotechnological materials. Such is the importance of these gene-keeping biomacromolecules that even nanomaterials have succumbed to the claimed benefits of DNA and RNA. Currently, there could be found in the literature a practically intractable number of examples reporting the use of combination of nanoparticles with nucleic acids, so boundaries are demanded. Following this premise, this review will only cover the most recent and powerful strategies developed to exploit the possibilities of nucleic acids as biotechnological materials when in combination with mesoporous silica nanoparticles. The extensive research done on nucleic acids has significantly incremented the technological possibilities for those biomacromolecules, which could be employed in many different applications, where substrate or sequence recognition or modulation of biological pathways due to its coding role in living cells are the most promising. In the present review, the chosen counterpart, mesoporous silica nanoparticles, also with unique properties, became a reference material for drug delivery and biomedical applications due to their high biocompatibility and porous structure suitable for hosting and delivering small molecules. Although most of the reviews dealt with significant advances in the use of nucleic acid and mesoporous silica nanoparticles in biotechnological applications, a rational classification of these new generation hybrid materials is still uncovered. In this review, there will be covered promising strategies for the development of living cell and biological sensors, DNA-based molecular gates with targeting, transfection or silencing properties, which could provide a significant advance in current nanomedicine.

Received 30th November 2016,
Accepted 30th December 2016

DOI: 10.1039/c6bm00872k

rsc.li/biomaterials-science

1. Introduction

The development of nanotechnology has significantly increased the number of possibilities for many biological tools. For example, the use of nucleic acids in nanohybrids is destined to become of great importance because it may allow combining, in a single entity, the biotechnological potential of nanoparticles together with the recognition, sensitivity or gene modulation abilities of nucleic acids when applied to living organisms.

Moreover, the use of nanoparticles as core platforms for those devices could provide novel and interesting hybrids as detection, diagnosis and/or therapeutic effect features to these devices,[1–3] which are two fundamental applications of nanoparticles in biotechnology. Related with cancer, nanometre sized particles offer a unique platform for the development of both therapeutic and diagnosis devices. This effect obeys the particular physiology of solid tumours, which produce interactions with nanoparticles and macromolecules in a very particular way, leading to the spontaneous and preferential accumulation, within the tissue, of those particles. This occurs because of the uncontrolled, high and anarchic vascularization of tumours, which produces fenestrations and irregularities that generate aberrant morphologies, which facilitates the accumulation of these within the tumour. Moreover, the associated fast growth results in poor lymphatic drainage, which impedes correct elimination and clearance from the tissue. This combined phenomenon, known as the Enhanced Permeation and Retention (EPR) effect,[4–6] is responsible for turning nanoparticles into Trojan horses able to accumulate and attack solid tumours.

Of all the nanoparticles reported to date, Mesoporous Silica Nanoparticles (MSNs) are of great interest because they show

Dpto. Química Inorgánica y Bioinorgánica. Facultad de Farmacia, Universidad Complutense de Madrid. Plaza Ramon y Cajal s/n. Instituto de Investigación Sanitaria Hospital 12 de Octubre i+12, Centro de Investigación Biomédica en Red de Bioingeniería, Biomateriales y Nanomedicina (CIBER-BBN), Madrid, Spain. E-mail: vallet@ucm.es

good bioactivity and biocompatibility and a unique porous structure in the nanometre range. This particular morphology allows the hosting of significant amounts of small molecules,[7] chemotherapeutics[8] or even macromolecules, thus opening the door for the development of drug carriers and nanodevices for intracellular detection.[9–11] Moreover, and contrary to other nanoparticles, MSNs offer intrinsic advantages like an outstanding chemical modularity, robustness and biodegradability.[12–15] Despite their huge potential for the development of carriers, the use of MSNs is still far from extensive clinical application. This is partly a consequence of an incomplete knowledge of MSNs in terms of chronic toxicity, long-term biodistribution, excretion, optimal size and morphology. It too is a consequence of the development of advanced systems itself, which usually include non-evaluated chemical species to provide better drug release profiles, which may compromise the potential use of the generated devices. A good example of this effect could be found in the development of molecular gates for MSNs[16,17] whose laudable purpose of drug carriage or retention of therapeutic drugs could be medically limited by the extensive use of non-biogenic compounds of broad nature (polymers, sensitizers, linkers, cytotoxics, other nanoparticles, *etc*.). Moreover, the incorporated sensitivity to a variety of stimuli (pH, temperature, glutathione, *etc*.)[17] may lead to unexpected, remainder, potent and persistent side effects (accumulated xenotoxicity, enhanced sensitivity to components or uncontrolled physiological responses, *etc*.). Thus, to avoid those issues, an important effort has been made by researchers to introduce biocompatible compounds to reduce the impact of the advanced MSN based nanomedicines. Because of this, the interest in sustainable and biogenic materials is growing and gathering attention from the scientific community. Indeed, the functionalization of MSNs with nucleic acids (NAs) not only would provide reduced toxicities, but also could provide additional and interesting features derived from their biological processes such as gene coding or intracellular signalling processes. Furthermore, their specificity towards complementary strands, high chemical stability and robustness together with the possibility of custom synthesis and amplification through highly developed processes make nucleic acids outstanding materials for the development of numerous applications. For example, some additional and remarkable features achieved by the incorporation of nucleic acids into MSN platforms are aptamer-mediated active vectorization, construction of stimuli-responsive molecular gates, carriage of gene modulators and development of advanced sensors, which will be reviewed in detail.

2. Pore gating by DNA in mesoporous silica nanoparticles

The unique porous structure of MSNs allowed the development of loadable nanosystems able to host small molecules, which resulted in the development of promising applications like drug delivery agents for cancer treatment,[8,18,19] platforms for catalysis,[20–22] sensors[23,24] and other biotechnological devices.[25–27] Despite their huge potential for biomedical applications, their use as raw material for drug delivery presents a major problem, the burst-type uncontrolled release of loaded compounds from the pores when in suspension.[7] This undergoes massive leakages, which reduce significantly the cargo efficiency and thus the possible therapeutic effect. For this reason significant effort has been made to develop different responsive systems able to efficiently retain the loaded compounds.[10,17] Among all the different nanogates developed, extensively reviewed by Martínez-Máñez and coworkers,[17] our interest would be focused only on the use of nucleic acids, particularly DNA. The use of NAs for this purpose presents significant advances such as biocompatibility, custom synthesis, length variability and chemical stability, huge sensitivity towards complementary sequences, recognition abilities and gene modulation roles. Regarding the topic of interest, three different strategies for the development of DNA-based nanogates onto MSNs could be clearly identified in the literature.

2.1 Electrostatic deposition of DNA strands onto MSNs

The first strategy, developed by Martínez-Máñez and coworkers, is based on the electrostatic deposition of the naturally negatively charged DNA strands onto positively charged MSNs.[28] In this system the authors functionalized raw MSNs with 3-(aminopropyl)triehoxysilane (APTES) to provide the positive charges (1.98 mmol g^{-1}) able to achieve electrostatic deposition. The chosen oligonucleotide 5′-(AAT GCT AGC TAA TCA ATC GGG)-3′ (0.022 mmol) was then employed for coating and proved to effectively retain fluorescein into the pores with an accumulated leakage of about 10% when in the closed state (Fig. 1). The authors tested satisfactorily the complementary strand as the opening stimulus for their model. This strand was able to seize the blocking strand from the MSNs, thus removing the pore protective layer by hybridization, thus allowing the release of loaded fluorescein. Although this model is not suitable for *in vivo* applications because it needs a complementary strand for triggering the nanovalve, it established the basis for complementary DNA displacement release (section 3.2) and polyelectrolyte deposition (section 4), which have been widely employed by other research groups as will be reviewed below.

In a recent upgrade of the state-of-the-art in electrostatic deposition of DNA onto MSNs, Ren, Qu and coworkers reported a multi-responsive device with great potential for the

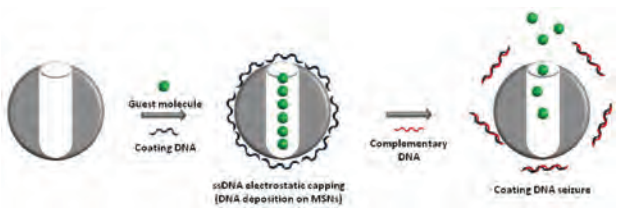

Fig. 1 Capping MSNs with DNA through electrostatic multilayer deposition.

treatment of cancer. Their design employed DOX-loaded cationic MSNs, which were efficiently capped with the C-rich sequence 5′-(CCC TAA CCC TAA CCC TAA CCC)-3′.[29] In their investigations they demonstrated that the chosen sequence was sensitive to nucleases, like telomerases, thus producing chemical degradation (see section 5.3). Moreover, the designed stand is also sensitive to pH shifts due to the formation of a C-rich quadruplex (see section 2.3), which produces strand self-folding and thus a worse capping. As those two effects are usual in cancerous cells, this device could lead to the generation of a novel family of therapeutic devices able to respond to the particular intracellular environment of cancer tissues.

2.2 Gates for mesopores based on double stranded DNA

The second strategy reported for the construction of capping valves onto mesoporous materials employing DNA was initially reported by Bein and coworkers[30] and was soon improved in a contribution by Vallet-Regí and coworkers.[31] These approaches demonstrated that single strands produce an ineffective pore capping while hybridized double strands conveniently placed on the pore surrounding do effectively block the diffusion. In both reported examples, the triggering stimulus was the thermal mediated dehybridization of double stranded DNA (dsDNA). Both pairing DNA sequences were then carefully designed to produce thermal dehybridization in a biocompatible range of temperatures. The submission of both nanodevices to the programmed melting temperature caused the dehybridization of the dsDNA, which could be assumed from the release of the loaded model molecules from the silica mesopores. In these examples, and contrary to the previous model, the DNA is directly grafted to the surface of the MSN through covalent bonds and the complementary pairing strand hybridizes this anchor strand. In both cases, the capping efficiency was in concordance with the common estimated values for common MCM-41 type mesopores (in the range of 2.5 to 3.0 nm) and the thickness of dsDNA (around 2 nm).[32]

In the model reported by Bein, 50 nm average diameter MSNs were functionalized with an azide group which was grafted to either 15 or 25mer DNA strands through click chemistry. The demonstration of ssDNA hybridization was done through FRET experiments employing two labelled strands with Cy3 and Cy5 respectively. The double-stranded system, when excited with Cy3 adsorption wavelength, produced typical Cy5 emission spectra due to the FRET effect. This clearly proved that the proximity of both dyes (less than 10 nm) was a direct consequence of an effective hybridization of DNA strands. Once hybridization was demonstrated, the authors evolved the system including biotin and avidin functionalized oligonucleotides to increment the bulkiness within the pore area for capping improvement[30] (Fig. 2). In a contribution by the group of Vallet-Regí, magnetic nanoparticles were employed to build a double-stranded, thermal-responsive system. In this design, amino modified magnetic MSNs were decorated with a ssDNA using the bifunctional linker sulfoSMCC, which afforded 60% substitution of the amino groups with the anchor strand. The counterpart, Fe_3O_4 nanoparticles grafted to the complementary strands, were responsible for both improving the capping efficiency and acting as magnetic stimulus sensitizers. The chosen pairing strands 5′-(HS-TTA TCG CTG ATT CAA)-3′ were designed to melt within the range of 47 °C, which is easily reached through magnetic induction and coincides with the upper limit of therapeutic hyperthermia in cancer therapy.[33–37] Release studies accomplished on this model showed a temperature dependent exponential release of the loaded fluorescent probe and an interesting reversibility of the capping particle produced by the rehybridization of both DNA strands when the thermal magnetic induction arrests (Fig. 2). This last strategy proved to be suitable for the controlled release of cargoes upon the application of highly controllable external stimuli such as alternating magnetic fields (AMF). More recently, an implementation of this idea was reported by Zhu and Tao, who improved the capping efficiency of the double stranded DNA by using multiple-point anchoring.[38] Hence in an implementation of this last device, similar magnetic Mesoporous Silica Nanoparticles (mMSNs) were bound through a maleimide–succinimide bifunctional linker (sulfoEMCS) to the anchor single strand 5′-(HS-$(CH_2)_6$-TTA TCG CTG ATT CAA)-3′ as was previously done.[31] However the authors employed a double sized, symmetric complementary strand 5′-(TTG AAT CAG CGA TAA TCG AAT AGC GAC TAA GTT)-3′ capable of double interactions with the anchor strands. Their studies with DOX as a loaded molecule showed an accelerated release when the pH was set to 5 and the temperature was set to 50 °C, which was obtained for a 50 mg mMSNs per mL sample at alternating frequencies of 409 kHz at either 150 Gauss for 20 min or 180 Gauss for 10 min. Moreover, this example undoubtedly proved the initial postulate of capping only with hybridized DNA strands, as no bulky compounds were required for effective pore blocking.

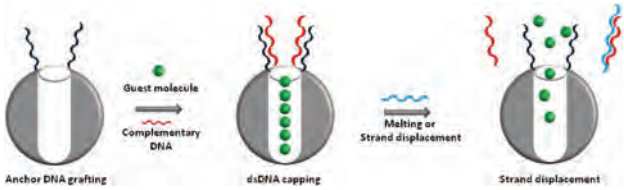

Fig. 2 Capping mesopores using the double strand hybridization approach.

As will be overviewed below, the use of dsDNA as pore gates is a highly versatile tool, as their dehybridization could be also triggered by other chemical or biological stimuli such as pH, specific DNA sequences or even enzymes (section 5.4).[24] The first example of a pH-driven nanogate was reported by Chen *et al.*; in this work robust amide bonds were employed to bind the 5′-($H_2N(CH_2)_3$-ATT GCA GGG TTA GTG)-3′ sequence onto MSNs. Then, the partially complementary i-motif containing strand 5′-(TCC CTA ACC CTA ACC CTA ACC CTG CAA T-$(CH_2)_6$-SH)-3′ was hybridized to the anchor strand producing the pore capping. The chosen i-motif DNA sequence is able to change its conformation from linear to a self-folded quadruplex when

the pH decreases. This resulted in a system that was able to remain closed when in basic pH and could be opened when in acidic media.[39] Additionally, in this example the authors enhanced the capping properties by using bulky Au nanoparticles bound to the terminal thiol groups at the 3′ end of the i-motif DNA.

Another reported stimulated release is the displacement of capping DNA by a specific complementary strand. This was elegantly demonstrated by the group of Martínez-Máñez in several research articles.[28] In another relevant example there was designed a dsDNA gated nanosystem able to dehybridize in the presence of particular DNA sequences.[40] In their model the 5′-(NH_2-$(CH_2)_6$-GAC TAC CAG GGT ATC)-3′ sequence bound to MSNs produced hybridization with the partially complementary 5′-(AAG CGT GGG GAG CAA ACA GGA TTA GAT ACC CTG GTA GTC)-3′ sequence, thus achieving efficient pore capping for rhodamine B fluorophore. In this case the responsive stimulus for the gate was the genomic content of *Mycoplasma fermentans*, which effectively displaced the capping strand, thus releasing the loaded dye. Indeed, the extraordinary recognition ability of DNA towards their complementary strands made this system only responsive to *Mycoplasma* and not to other common pollutants such as *Candida albicans* or *Legionella pneumophila*. These systems, although more suitable to be reviewed in the MSN–DNA hybrids with sensing properties (section 5), were introduced here to demonstrate the potentiality of this strategy.

2.3 Nanogates based on DNA quadruplexes

The third approach to build nanovalves onto mesopores is based on the use of a self-foldable duplex or quadruplex DNA architecture. Briefly, for this strategy is placed heavily folded single stranded DNA duplexes in the pore vicinity, which are able to block the diffusion through the pores. Hence, the exposure of those duplexes to an adequate stimulus induces unfolding and a subsequent unconstrainment of the pore surroundings, thus facilitating the diffusion of compounds from the pores. This strategy, developed by Qu and co-workers, was the first to introduce stimuli-responsive DNA sequences for reversible pore caping.[41,42] In one example the authors prepared DNA–MSN hybrids bound through amide bonds using the 5′-(H_2N-$(CH_2)_6$-CCC TAA CCC TAA CCC TAA CCC)-3′ sequence as pH dependent quadruplex strands. According to the published results, the fluorescent probe rhodamine B was efficiently retained within the pores at pH = 5, where the duplex is favoured and released at pH = 8, where the expanded conformation prevailed.[41] In an almost simultaneous contribution, the same group reported the use of the DNA duplex forming strand 5′-(GCA TGA ATT CAT GC)-3′ to modify MSNs[42] in order to build temperature dependent and reversible pore gates; for this gating the authors employed the previously developed click methodology[30,43] (Fig. 3).

Based on the quadruplex-folding, a pore capping pH-dependent conformational shift was reported by Wang's group, who developed a UV light triggered valve onto MSNs.[44] This was based on both the i-motif DNA able to change its conformation upon pH variations and the malachite green carbinol base (MGCB), with known hydroxyl releasing properties upon irradiation with UV light.[45] In order to produce the necessary conformational switch between the packed quadruplex and expanded strand, the photo-responsive pH-shifter MGCB was loaded within the pores to induce a maximal effect over the i-motif DNA located in the outer region of pores. Pore capping, MGCB loading and pore opening were studied and confirmed from N_2 adsorption data. For the construction of this system the authors chose click chemistry to anchor the quadruplex forming strand 5′-(HC≡CH-$(CH_2)_4$-CCC TAA CCC TAA CCC TAA CCC)-3′ to the MSN surface, reaching a functionalization of up to 4.3 μmol g^{-1} SiO_2. More recently this research group evolved their initial design to build a cation-dependent responsive gate for MSNs.[46] For this, they employed a sequence that reverts its packed conformation in the presence of K^+ cations to a random one in the presence of Ag^+, 5′-(HC≡CH-TGG GTA CGG GTT GGG AAA)-3′. This gate also proved to be reversible in the presence of thiols, thus being able to open or close the gate on demand by alternating Ag^+ and Glutathione-SH (GSH) or even with the biogenic amino acid cysteine. Other systems able to behave as cation sensors are detailed in section 5.3.

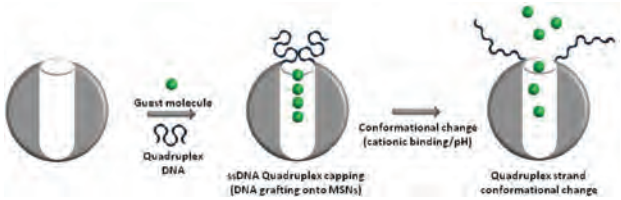

Fig. 3 Capping MSNs with DNA through G-quadruplex forming strands.

Another interesting example of a light triggered pore opening process based on G-quadruplexes was reported by Ren, Qu and coworkers.[47] In their design they employed the 5′-(HC≡C-$(CH_2)_4$-TTG GGG TTT TGG GG)-3′ dimeric quadruplex forming sequence to efficiently cap the mesopores through a click process, while, on the other hand, to obtain the light sensitivity property, the authors intercalated in between the dimer folded quadruplex strands a 2 molar ratio of the *meso*-tetra(*N*-methyl-4-pyridyl)porphine tetratosylate ($TMPyP_4$) photosensitizer. This, able to generate ROS species upon illumination, induced chemical degradation of the DNA, thus reverting the quadruplex folding and producing fluorophore release from the mesopores. Moreover, the authors provided interesting information about the size of the different counterparts involved in pore retention and release processes. Indeed they employed MSNs bearing regular 2.9 nm mesopores and 1.5 nm rhodamine fluorophore, which proved to efficiently diffuse through those channels. However, the later functionalization of the particles' surface with the quadruplex DNA tetrad (2.0 nm thick) hampered enough the pore diffusion to effectively retain the model fluorophore until light stimulation.

2.4 Double stranded gates based on DNAzymes

The concept DNAzyme refers to those single stranded DNA (ssDNA) oligonucleotides able to perform catalytic reactions in a similar way to known enzyme–substrate examples. Their catalytic activity thus relies on the three-dimensional structure induced by the G-quadruplexes present in the sequence, which folds the structure like in enzymes. Indeed there have been also reported examples where those ssDNA behave as holoenzymes and require from cofactors to perform its activity.[48–51] Since their discovery, DNAzymes have been widely exploited in medicine, biology and materials sciences because of their advantages over conventional enzymes, which are principally a higher thermal stability and simpler preparation. Unlike enzymes, responsible for a huge number of processes, known processes catalysed by DNAzymes are limited, although efficiently catalysed.

Hence, for the topic we are focused on, DNAzymes have opened the door for the development of interesting DNA–MSN gated devices. To turn those sequences into gating mechanisms there are two fundamental requirements: first, that the DNAzyme is able to remain inactive until exposure to an activation stimulus and, second, the presence of a substrate able to act as a cleavable moiety. The first aspect is simple to control as usually DNAzymes require a metallic cofactor(s) (Cu^{+2}, Cu^{+2}/Mn^{+2}, Cu^{+2}/Zn^{+2}, *etc.*) to be catalytically active. The second requirement, which seemed unbridgeable, has been elegantly solved by the use of DNAzymes with nuclease activity. Those particular sequences bearing cleavable points are the perfect candidates for the development of triggered systems in which the release of the capping double strand produces the pore opening[51] (Fig. 4).

This strategy to build nanogates was recently developed by the group of Willner. In their first contribution the authors employed sulfoEMCS as a cross-linker to link the MSNs with the cleavable 5′-(6-HS-CAA CAA CAT *r*AGG ACA TAG AAG AAG AAG)-3′ sequence (the cleaving point is denoted by *r* for clarity), which is known to be a substrate for both Mg^{+2} and Zn^{+2} dependent DNAzymes[52–54] through the cleavable T*r*AG sequence. The system was then loaded with methylene blue (or thionine) and closed with the complementary DNAzyme-containing sequences 5′-(CTT CTT CTT *CTA TGT CAG CGA TCC GGA ACG GCA CCC ATG* TTG TTG TTG)-3′ sensitive to Mg^{+2} or with the Zn^{+2} dependent sequence 5′-(CTT CTT CTT *CTA TGT CTC CGA GCC GGT CGA AAT G*TT GTT G)-3′. This design proved to be an efficient and cation-dependent pore gate because the enzymatic activity of the DNAzyme could be only recovered if the adequate cofactor was present.[55] More recently, the same research group demonstrated the potency of this strategy by reporting an evolved version of this methodology in which the cation-dependent release system is also sensitive to pH.[56] In this model the cleavable T*r*AG trinucleotide containing sequence 5′-(HS$(CH_2)_6$-CAG TGA ATT *r*AGG ACA TAG AAG AAG AAG)-3′ was grafted onto the MSNs pore proximity employing the reported methodology (1.8 μmol DNA per g MSNs). Then, the Mg^{+2} dependent 5′-(CTT CTT CTT CTA TGT CAG CGA TTC CGG AAC GGA CAC CCA TGT ATT CAC TG)-3′ or the UO_2^{+2} dependent 5′-(CTT CTT CTT CTA TGT CAG CCG GAA CGG CCT TGC AAT TCA CTG)-3′ strands were used to close the pores through hybridization. However, on these models, pH is also a pivotal parameter to control the activity of DNAzymes, as acidic pH enhances the catalytic activity of the UO_2^{+2} dependent DNAzyme, while neutral pH keeps it inactive and does not produce release. On the other hand, the Mg^{+2} dependent DNAzyme shows the opposite behaviour, remaining inactive under an acidic environment and active under neutral conditions.

As will be reviewed in the next sections, all the different reported responsive gates for MSNs are aligned with two research lines. The first, nanomedical research, mostly profits from the capping strategies based on macromolecule recognition and physically-triggered stimuli, while the development of smart materials for sensing applications shows a clear preference for chemical stimuli such as pH or the presence of certain cations or small molecules.

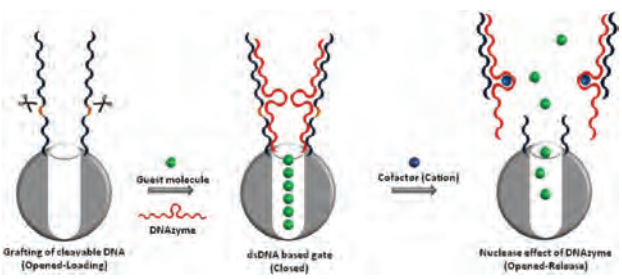

Fig. 4 Loading–release mechanism of DNAzyme-based gates.

3. Aptamer functionalized mesoporous silica nanoparticles

Contrary to other biogenic nucleotides such micro-RNAs (mRNAs), which are responsible for transcription of genetic information, or small interfering RNAs (siRNAs), which interrupt such a transcription, aptamers are synthetic, single-stranded short oligonucleotides (from 20 to 80 bases) without any coding information but with a well-formed three-dimensional structure that allows a high affinity interaction with their target molecules, proteins or cellular receptors.[58] Added to their extraordinary recognition ability, aptamers also show particular features that turn them into valuable candidates for nanotechnological applications. Some remarkable advantages are their low immunogenicity, a well implemented synthesis, relatively small size, flexibility, excellent biocompatibility and the possibility of chemical modification very useful for functionalization purposes.[59] Moreover, aptamers, contrary to proteins, are not denaturalized under thermal shocks because they are able to refold to their active three-dimensional configuration once heating arrests,[60] thus maintaining their recognition properties. Aptamers are obtained by a process called Systematic Evolution of Ligands by Exponential Enrichment (SELEX), which is briefly a combinatorial process in which

different chains of oligonucleotides (primers) are polymerized in the presence of a target molecule or structure. Then, among all the random sequences obtained, the strands with higher affinities will remain tightly bound to the template after polymerization,[61,62] so it is possible to discard non-specific unbound sequences by washing out. Through an iterative process of polymerization, affinity elution and amplification, the final aptamer is selected and thus evolved among all the possibilities obtained. This technique generates specific sequences able to fit the template compound with affinities comparable to that of antibodies. Indeed, this powerful process is able to generate selective aptamers for almost any chemical entity,[63] which enables the possible recognition of important biomarkers. For example, only focusing on nanovehicles with anticancer purposes, there have been reported many different examples with good specificity able to match different bioactive receptors of different cell lines (Table 1).[57] In general, aptamers have been widely employed for drug delivery strategies[57] in many different platforms such as aptamer–drug conjugates,[64,65] polymeric-based nanoparticles,[66] liposomes,[67] hard inorganic nanoparticles[68,69] or even chimeras.[70] Nevertheless, aptamers have also a great impact on mesoporous silica nanoparticles, because besides the traditional targeting they also offer interesting features such as pore gating.

From here on, a clear distinction between MSNs–aptamer hybrids will be made. In the following sections our interest will be focused on the recognition of cellular biomarkers and membrane proteins by aptamers, that is, active targeting in nanomedical applications. Later, in a further section, our interest will be shifted to recognition and detection of small molecules for sensing applications (section 5).

3.1 Aptamer–MSNs hybrids for active targeting

Among all the reported aptamers developed for biorecognition, AS1411 is by far the most widely employed as it was the first to enter clinical trials,[71] the reason why most of the reported delivery models use this aptamer as the targeting moiety. Although obtained by serendipity, its mechanism of action is nowadays is properly settled and its effect on cancerous cells is also well known.[72] The AS1411 aptamer targets nucleolin (NCL), a eukaryotic nuclear protein, commonly located at the nucleolus, which is involved in ribosomal maturation. However, many cancerous cell lines show this protein overexpressed in their cellular membranes, which turns NCL into a valuable biomarker and an adequate candidate for targeted anticancer therapies.

In the first aptamer-targeted example developed onto MSNs, an elongated version of the NCL aptamer 5′-(*GGT GGT GGT GGT TGT GGT GGT GGT GGT* TTT TTT TTT-SH)-3′ was employed as a recognition moiety. In this model MSNs were functionalized with amino groups, which were incorporated into the raw phosphonate-MSNs by functionalization with APTES.[73] The later linkage to the oligonucleotide was achieved by employing the bifunctional linker sulfoSMCC, which bound both the aptamer and MSNs through the respective thiol and amino groups present in each subunit. With this approach the aptamer grafting efficiency reached values up to 1.5 mmol DNA per g MSN. This was then confirmed by IR spectra thanks

Table 1 Nanoparticle targeted aptamers for drug delivery. Adapted from ref. 57 and updated for this review

Aptamer	Number of bases	Target[a]	Cell line(s) tested	Vehiculization[b]	Drug(s) loaded[c]	*In vitro*/*in vivo*
AS1411	26–28 (DNA)	Nucleolin (NCL)	MCF-7, PANC-1, PC3, MDA MB-231	PLGA, liposomes, CNT, MSNs*	DOX, PTX	Y/Y
A10	57–91 (RNA)	PSMA	LNCap, CWR22Rv1	Micelles, PLGA	DOX, Pt, DTX	Y/Y
SZTI01	48 (DNA)		C4-2	Aptamer–drug hybrid	DOX	Y/N
5TR1	25 (DNA)	MUC1	C26	Aptamer–SPION	EPI	Y/Y
MA3	86 (DNA)		A549, MCF-7	Aptamer–drug hybrid	DOX	Y/N
—	25 (DNA)		CHO-K1, MCF-7	DNA chimera	DOX	Y/N
S2.2	19 (DNA)		MCF-7, HepG2	PLGA	PTX	Y/N
—	25 (DNA)		A2780/AD	QD–Aptamer–DOX hybrid	DOX	Y/Y
Sgc8c/sgc8	41–48 (DNA)	PTK7	CCRF-CEM, Ramos, HCT116, Molt-4, U266	PLGA, CNT, MSNs*, Aptamer–drug hybrid	DOX, PTX, 5FA, DNR	Y/Y
Ploy-Apt	41 (DNA)		CCRF-CEM, Ramos	Aptamer–drug hybrid	DOX	Y/N
—	14 (RNA)	EpCAM	HT 29, HEK293T	PLGA	CUR	Y/N
EpDT3	19 (RNA)		Y79, WERI-Rb1	Aptamer–drug hybrid	DOX	Y/N
—	48 (DNA)		SW620, Ramos B	MSNs*	DOX	Y/N
DDSs	48 (DNA)	Cyt c	HeLa	AuNRs@MSNs	ROT	Y/N
—	39 (RNA)	CD30	Karpas 299, SUDHL-1	Hollow AuNPs	DOX	Y/N
TLS11a	63 (DNA)	LH86	LH86	Aptamer–drug hybrid	DOX	Y/Y
HB5	86 (DNA)	HER2	SK-BR-3, MDA-MB-231, MCF-7	MSNs*, Aptamer–drug hybrid	DOX	Y/N

Abbreviations: [a]PSMA, prostate-specific membrane antigen; MUC1, mucin 1; PTK7, protein tyrosine kinase 7, EpCAM, epithelial cell adhesion molecule; Cyt c, cytochrome c; CD30, tumour necrosis factor receptor superfamily 8, HER2, human epidermal growth factor receptor 2; [b]PLGA, poly(lactic-*co*-glycolic)polymer; CNT, carbon nanotubes; MSNs, mesoporous silica nanoparticles; SPION, superparamagnetic iron oxide nanoparticles; QD, quantum dot; AuNPs, gold nanoparticles; AuNRs, gold nanorods; [c]DOX, doxorubicin; PTX, paclitaxel; DTX, docetaxel; EPI, epirubicin; 5FA, 5-fluorouracil; DNR, daunorubicin; CUR, curcumin; ROT, rotenone. *Reviewed below.

to the detection of imidyl and amide vibration bands. The aptamer grafting onto MSNs was confirmed by an elegant hybridization essay employing complementary strands bound to Au nanoparticles. In the case of base-matching, this is perfect complementarity, there was generated a raspberry-like structure of AuNPs surrounding the central MSNs. While in the case of poor complementarity, this structure could not be obtained. The resulting aptamer-targeted system was loaded with doxorubicin (DOX) as cytotoxic drug and was evaluated against NCL-positive MCF-7 breast cancer and NCL-negative LNCaP prostate cell lines. The published results showed preferential accumulation into breast cancer cells with a subsequent increase on their mortality. In a parallel design, the epithelial cell adhesion molecule (EpCAM) aptamer 5′-(H_2N-*CAC TAC AGA GGT TGC GTC TGT CCC ACG TTG TCA TGG GGG GTT GGC CTG*)-3′ was reported for the targeted delivery of DOX to colon cancer cells using MSNs.[74] This system, tested against human SW620 colon cancer cells and Ramos B lymphoma cells demonstrated a cytotoxic effect on both cell lines, but with a preferential accumulation and thus an enhanced therapeutic effect on the colorectal cell line.

In a nice implementation of the aptamer targeted delivery of MSNs, Li *et al.* designed a nanosystem in which the active targeting of aptamers was complemented with an elegant intracellular triggered drug release. In their design there were employed desthiobiotin (DTB) modified sgc8 aptamer strands 5′-(desthiobiotin-TTT TTT TTT *TAT CTA ACT GCT GCG CCG GGA AAA TAC TGT ACG GTT AGA*)-3′, able to specifically recognize the protein tyrosine kinase 7 (PTK7) which is overexpressed in lymphoblastic leukaemia cell lines. For the design of the disintegrable cap the authors employed DTB functionalized MSNs, which upon linkage with avidin (AV), provided an aptamer ended, avidin bridged structure (MSN-DTB-AV-DTB-Sgc8).[75] This system thus combined in a single device the recognition ability of the aptamer with the pore blockage exerted by the avidin–desthiobiotin protein complex. The opening mechanism was mediated by biotin which could effectively displace the analogue DTB from the avidin complex. As biotin is a compound mainly located on intracellular environments, the disassembly was only produced upon cellular uptake, thus minimizing uncontrolled leakage of the loaded drug. The viability studies showed increased mortality for the targeted device, what points towards a higher internalization and intracellular DOX release. On the non-targeted devices, both gated and non-gates devices showed similar viabilities, probably due to a poor uptake and a similar intracellular release profile.

The interest in controlling the stimulus in gated materials is of great importance as it may give access to controlled or even upon-demand releases of the loaded species. Unfortunately this is an extremely complex task, mostly when the triggering effect relies in biological or endogenous parameters (pH, reducing power or the presence of certain compounds), because they are difficult to control and to maintain within the optimal action range. Then, unless the systems are specifically tuned to meet a very precise intracellular conditions, external stimuli are usually preferred because of important advantages like the ease of application and the time/intensity control. Two of the most recurrent stimuli for these purposes are the thermal induction, which employs alternating magnetic fields (AMF) with magnetic materials[3,34] and light induced photothermal (PTT) effect for materials bearing photoactive compounds. Those could be of a broad nature, for example inorganic species as upconversion particles[76,77] or gold based materials[78] or organic materials such as graphene, porphyrins or conjugated polymers.[79–81] Nevertheless, the current tendency for the study of thermal induction effects seems to be currently shifted to plasmonic and photothermal materials, as they do not require from the expensive infrastructure needed to achieve magnetic induction heating. Upon this basis, there have been developed several aptamer-targeted devices that exploit the external application of light stimulus to induce pore uncapping and drug release; which are mainly based on plasmonic heating of Au.

In the contribution by Ren, Qu and co-workers, there were employed mesoporous silica nanoparticles which embedded gold nanorods (AuNR@MSNs); a structure sensitive to near Infrared (NIR) which is able to produce plasmonic heating. These particles were functionalized, through amide bonds, with the anchor strand 5′-(NH_2-$(CH_2)_6$-TGG TCT ACT TGA)-3′, which was able to hybridize elongated strands of NCL aptamer 5′-(*GGT GGT GGT GGT TGT GGT GGT GGT GGT* CAA GTA GAC CA)-3′. This additional 12-base elongation, resulted in an effective pore blockage due to dsDNA hybridization, while maintained unaltered the recognition ability of the aptamer.[82] The gate opening was effectively achieved with NIR irradiation (808 nm, 1.2 W cm^{-2}) which was able to heat plasmonically the AuNR embedded within the MSNs, thus producing light-assisted dsDNA melting and the expected opening.

Although cellular membrane proteins are by far the most common target for reported aptamers, other important biomacromolecules showed also promising results. For example, in other contribution by Qu and co-workers, Cytochrome c specific binding aptamer 5′-(*CCG TGT CTG GGG CCG ACC GGC GCA TTG GGT ACG TTG TTG CTT* TTT TTT-SH)-3′ was employed to target mitochondria using the previously employed AuNR@MSNs.[83] In this model, Rotenone was used (ROT) as specific inhibitor of the mitochondrial activity. The authors demonstrated a clear potentiation of the apoptotic effect when activity disruption of this critical organelle was induced; as expected the combination of chemo- and photothermal effects also had a synergic effect on the reduction of cell viability.

Other interesting examples of combination of chemo-photothermal effects based on carbon were reported almost simultaneously by two research groups. In one example, reported by Wang *et al.*, the human epithelial growth factor receptor 2 (HER2) HB5 aptamer 5′-(*AAC CGC CCA AAT CCC TAA GAG TCT GCA CTT GTC ATT TTG TAT ATG TAT TTG GTT TTT GGC TCT CAC AGA CAC ACT ACA CAC GCA CA*)-3′ was successfully grafted onto DOX-loaded semi-graphitized carbon containing MSNs.[84] In this case the authors included PEG for stealthiness purposes although did not incorporate any gating

system onto the device; so the DOX release was then continuous and accelerated when pH decreased. Nevertheless, the evaluation of those HB5-modified MSNs *in vivo* against SK-BR-3 tumour-bearing mice showed a significant reduced toxicity. The authors justified this observed effect because of the targeting, which was able to reduce undesired accumulation on liver, kidney and especially in heart, as deduced form the fluorescence images. Furthermore when the system was exposed to the NIR laser combination therapy, a significantly decrease of cell viability was obtained in comparison to single therapeutic effects alone. On the sight of these results, the authors suggest that PTT heating could not only promote apoptosis induction but an enhanced dissociation of DOX–SiO_2 pair, thus reaching better therapeutic profiles.

The second example, reported by Tang *et al.*, employed MSNs wrapped with flexible graphene oxide (GO) nanosheets. In this model the authors profited from the properties of graphene to build a system able to transduce the near infrared (NIR) light into thermal energy. The system so designed was able to accomplish a triple function, first the GO layer was able to maintain the loaded DOX trapped in the pores, second it was able to retain the dye-labelled NCL aptamer 5′-(Cy5.5-T*TGG TGG TGG TGG TTG TGG TGG TGG TGG*)-3′ and third, quenched the Cy5.5 fluorescence.[85] As expected, the NIR irradiation (808 nm, 0.25 W cm^{-2}) induced local heating of the graphene nanosheets, producing a desorption process of silica and DNA from GO, allowing the release of the loaded drug. Reported results showed a clear synergic effect when chemotherapy and PTT were applied in combination, obtaining better results than individual chemotherapy or PTT alone.

As reviewed, aptamers have been widely successfully employed for providing recognition features to nanoparticles,[86–88] making them interesting for the development of many aptamer targeted devices. However, scientists' interests are shifting towards the development of simpler systems able to join together more DNA features onto advanced devices. One of those implementations could be the use of aptamers as gating moieties too.[89]

3.2 Aptamer–MSNs as responsive targeted devices

The use of aptamer functionalized MSNs opened a novel pathway to profit their advantageous recognition capabilities for the development of highly specific drug delivery platforms against cancerous cells. Nevertheless, this approach does not offer a solution for the continuous drug leakage which is one of the major drawbacks of the use of non-gated MSNs as nanocarriers. However, as previously commented, nucleic acids are also valuable components for the development of gated hybrids. Because of this, many different research groups have made important advances to combine in a single nanodevice both possibilities.

The first aptamer gated MSN-based system was reported by Zhu *et al.* In their approach there was employed a different strategy from those previously reported which took advantage of the highly specific recognition of aptamers. Their model was based on the use of two kinds of nanoparticles, one bearing an aptamer and the other functionalized with an analogue of the substrate. In particular, there were employed ATP-aptamer functionalized gold nanoparticles (AuNPs) and adenosine functionalized MSNs.[90] In this design the adenosine-5′-triphosphate (ATP) aptamer, 5′-(*CCT GGG GGA GTA TTG CGG AGG AAG GTT*-SH)-3′, was able to reckon the adenosine at the MSN surface; which produced a close and strong interaction between both MSNs and AuNPs and the consequent pore capping. In this device, the genuine substrate for the chosen aptamer, that is, ATP, was able to displace the bound adenosine from the aptamer. This caused the disassembly of the MSN–AuNP pair and the opening of pores. Indeed the extraordinary recognition ability of the aptamer employed made the system only responsive to ATP but insensitive to other similar compounds such as CTP, UTP or CTP (Fig. 5).

Another contribution based on the ATP aptamer recognition was reported by Wang and co-workers, who employed two different strands to hybridize simultaneously two different regions of the ATP aptamer. In this approach the nanogate was prepared prior to the grafting onto the nanoparticle's surface. First, there were hybridized the anchor DNA 5′-(TTC CTC CGC A)-3′, with the ATP aptamer 5′-(CAC CTG GGG GAG TAT TGC GGA GGA AGG TT)-3′ and the additional ssDNA 5′-(CCC TCA TA)-3′ to create a three-strand double helix with a favoured disassembly (10 base complementarity). On the other hand, the additional strand incorporated in the gate enhanced the capping of mesopores by increasing bulkiness at the pore vicinity.[91] The thus obtained sandwich-type triple oligonucleotide was grafted onto the MSN surface through click chemistry, resulting in pore closing with a DNA amount estimated to be about 1.6 μmol g^{-1} MSNs. Again, as in the precedent example, the presence of ATP is able to displace the aptamer from its hybrid strands, leaving only the short arm strands at the MSNs surface, which are unable to effectively block the pores (Fig. 6). These two proof-of-concept models based on the use of ATP as the releasing stimulus could be interesting for the development of ATP sensors (section 5.2) or for avoiding premature leakage while in the bloodstream, as release will only occur in intracellular environments. Nevertheless, because of its ubiquity, the ATP-mediated release would lead to unspecific pore opening, which reduces significantly its interest for biological applications.

Indeed, the use of an unspecific stimulus is not of interest for the current development of guided medicines. The use of

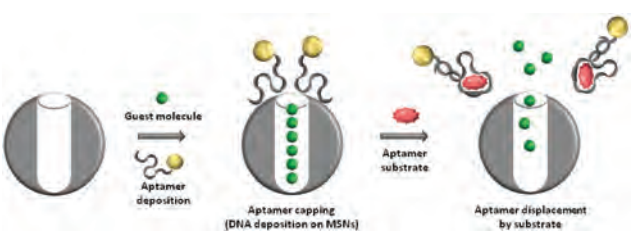

Fig. 5 Aptamer–MSNs nanogates based on electrostatic deposition. Adapted from ref. 89.

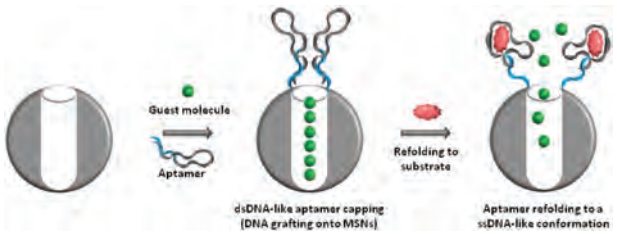

Fig. 6 Nanogates for MSNs based on self-foldable DNA aptamers. Adapted from ref. 89.

the extraordinary vectorization provided by aptamers, which are able to discriminate between healthy and cancerous cells, opens broad possibilities for the development of future nanomedicines. With this idea in mind Hernandez *et al.* designed an elegant evolution of the aptamer targeted MSNs in which the DNA itself is able to block the pores through self-folding.[92] For this approach the authors employed an enlarged oligonucleotide strand containing both the nucleolin sequence aptamer plus an additional region able to recognize partially the strand itself, 5′-(H_2N-CCA CCA C*GG TGG TGG TGG TTG TTG GTG GTG G*)-3′. This sequence proved to be hybridized at the pore environment as it was able to block the leakage of loaded 6-fluoresceinamidite (FAM) model fluorophore from MSNs. Furthermore, the recognition ability was maintained as the active hairpin aptamer structure is mostly kept unbound (bold sequence). The proposed mechanism of action in which the target nucleolin is able to induce dehybridization of the complementary 3′/5′-end double strand was demonstrated using the NCL-positive MDA-MB-231 and the NCL-negative MCF-10A breast cancer cell lines, showing a clear dependence between the presence of nucleolin and the release of the loaded fluorophore (Fig. 7, left).

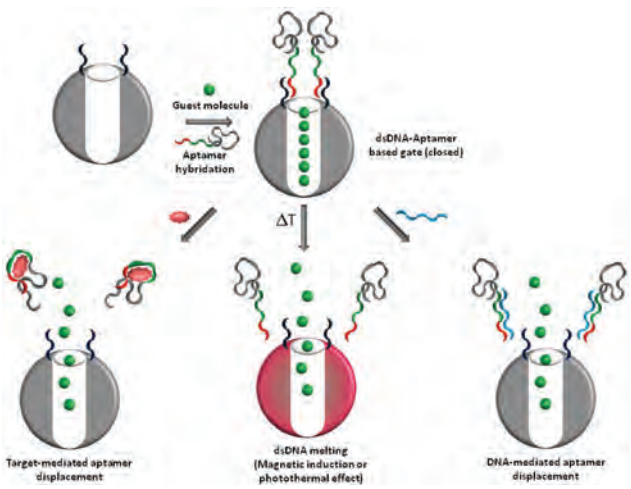

Fig. 7 Three different approaches for triggering release in aptamer containing dsDNA gates.

Another relevant strategy for the development of nanomedicine was reported by Zang *et al.*, who designed an interesting aptamer-targeted chemo-photothermal device for enhanced therapy. Their system employed photothermally active $Cu_{1.8}S$ nanocrystals embedded within a mesoporous silica matrix ($Cu_{1.8}S$@MSNs) to build a NCL-targeted carrier able to deliver both curcumin (CUR) and DOX simultaneously.[93] Here, the authors grafted the anchor strands 5′-(CGA CGA CGA CGA-SH)-3′ onto the $Cu_{1.8}S$@MSNs surface through the APTES–sulfoSMCC coupling methodology and loaded the mesopores with CUR. Then, the later hybridization with the aptamer-containing complementary strand 5′-(TCG TCG TCG TCG *GGT GGT GGT GGT TGT GGT GGT GGT GG*)-3′ formed the double stranded gatekeeper, which was employed to load DOX by intercalation. This approach combined, in a single carrier, two-drug co-delivery plus chemo-photothermal therapy, two of the most promising merging disciplines to reverse multi-drug resistance (MDR) in cancer. Reported studies showed again a preferential accumulation onto positive MCF-7 breast cancer cells and a poor uptake on the NCL-negative HEK-293 cells. Moreover, there was also reported an enhanced apoptotic behaviour when the three effects (CUR + DOX + NIR) were combined (Fig. 7, center).

As reviewed, recognition and hybridization abilities of aptamers have been successfully employed for the development of promising targeted gated materials. However, the use of DNA could also provide additional features like gene expression modulation. In an elegant example reported by Min, Zhu and co-workers, gene down-regulation was firstly introduced in a device in which an mRNA was the release stimulus.[94] This proof-of-concept is of great importance because the transcription of drug-resistance proteins is mediated by those mRNAs and their disruption may lead to new ways of arresting cancer proliferation and resistance. In this model the authors employed the well-known miR-21: 5′-(UAG CUU AUC AGA CUG AUG UU GA)-3′ as a release stimulus.[95] Then, once the target mRNA was chosen, the authors designed a dsDNA pore capping approach employing a 15-mer anchor strand sequence 5′-(HOOC-TTT TAG CTT ATC AGA)-3′ able to bind the 48-mer which contained the AS1411 and anti-miR-21 sequences: 5′-(*GGT GGT GGT GGT TGT GGT GGT GGT GG*T CAA CAT CAG TCT GAT AAG CTA)-3′. The system, in the presence of miR-21, is disassembled because this mRNA is able to displace the 48-mer AS1411/anti-miR-21 nucleotide from the 15-mer anchor strand (the pairing is denoted by a double underline) due to the formation a more stable 22 base-pair hybridization. This resulted in the consumption of miR-21 by its pairing with the AS1411/anti-miR-21 sequence and the immediate pore opening. In summary, there was designed an aptamer targeted, miR-21 triggered, DOX loaded carrier able to recognize the overexpression of NCL. Once internalized, the system was able to consume the antiapoptotic miR-21 while it released a cytotoxic drug. This resulted in a promising combined therapeutic effect in which the nucleic acids were responsible for three actions: targeting, capping and gene silencing (Fig. 7, right).

4. Transfection and gene therapy with mesoporous silica nanoparticles

Since their early beginnings, gene transfection and gene knockdown technologies have attracted great interest as they might enable control over most of the genetic diseases. The most recent technology, silencing RNAs (siRNAs), consists of the use of certain oligonucleotide sequences able to disrupt potently, persistently and specifically the normal effect of messenger RNAs on mammalian cells.

In cancer treatment, gene silencing is a promising therapy because the uncontrolled replication of cells usually has a genetic origin. Unfortunately, the negative charge, the big molecular size and the quick extracellular degradation of nucleic acids limit their use for direct application; nevertheless, nucleotides could be preserved from degradation when vectorization agents are employed. For this purpose viral vectors are not recommended because they present latent virulence or other side-effects. So, the development of nonviral vectors for gene silencing is a growing need in order to achieve a great gene therapy potential.[96–98] In fact, the ease, lower fabrication costs and the absence of immunogenic response of those nanomaterials could boost the applicability of nanomaterials in future gene and combination therapies.

Indeed, for these kinds of therapies a reversible linkage between nucleotides and nanocarriers is required. In this sense, MSNs could be tailored to fulfil those requirements from two different approaches. The first possibility is the development of electrostatic deposition of NAs onto the silica surface, whereas the second would profit from enlarged pore MSNs to host the nucleotides into their structure. As always, both approaches show advantages and disadvantages, but it is noteworthy that pore hosting would allow better delivery for highly sensitive compounds and may avoid undesired degradation.

4.1 Loading nucleotides into MSNs: new devices for transfection and gene therapy

The extraordinary ability of MSNs to load small molecules into their pores and the enormous potential for surface modification have allowed the development of a number of pore gated structures able to efficiently deliver drugs for different applications. Indeed MSNs are also interesting platforms for the development of macromolecule nanocarriers if expanded pore MSNs are employed.[99] Along this line there has been reported successful delivery of small proteins[100] and nucleic acids, which is the purpose of the current section.

The first study that introduced the loading of DNA into MSNs concept was reported back in 2005 by Fujiwara *et al.*, who had the pioneering vision that enlarged-pore silica nanoparticles could perform such a hosting.[101] In their investigations they employed different materials with pores in the range of 2.02 to 4.58 nm which were prepared by the rational variation of surfactants and incorporation of different additives throughout the synthesis. Unfortunately, they could not obtain clear evidence of pore filling. Nevertheless, there could be established two important salt-dependent governing mechanisms for DNA adsorption onto SiO_2. The first clear proof of DNA loading into MSNs was reported by Corma and co-workers employing 20.5 nm large pore MSNs (LP-MSNs).[102] Their particles were able to load DNA and protect it from external degradation although the quantity adsorbed was highly limited by a low particle size and a non-preferential adsorption between the pores and the surface.

After these initial efforts, Qin *et al.* set the parameters for the best hosting of DNA into mesopores, which was obtained with pores in the range of 8 to 10 nm, particularly, with 150 nm LP-MSNs with 9.8 nm pores. To facilitate the pore loading the authors coated the internal surface of pores with cationic poly(allylamine) moiety, while the external surface remained with its original negative charge.[103] This increased the affinity of the naturally negative DNA towards the pores, thus maximizing the loading efficiency. To assess the DNA loading into the pores, the authors employed the Green Fluorescent Protein (GFP) plasmid to evaluate its potential as a gene transfection agent. In their results, free plasmid was not able to transfect the cell while the plasmid-containing carrier could, which demonstrated the uptake and transfection potential of these pore loaded LP-MSNs.

Along this line, Steinbacher and Landry studied also the parameters that govern the loading and release of siRNAs from MSNs. For this, they employed different pore sized, tetraethyleneglycol (TEG) surface-capped MSNs, functionalized internally with variable amounts of the polycationic moiety diethylenetriamine (DETA).[104] In the light of their results, they claimed that short polyamine modifications like DETA were ideal to obtain high siRNA loadings; nevertheless, the degree functionalization must be carefully tuned as it plays a critical role. Indeed, for the chosen control siRNAs 5′-(GGG UAU CGA CGA UUA CAA AUU-AlexaFluor-647)-3′ and 5′-(UUU GUA AUC GUC GAU ACC CUG-AlexaFluor-647)-3′ (approximately 6 × 3 nm), it was found that larger pores showed higher loading ratios, although for the achievement of a loading–release reversible process, intermediate pore sizes and degrees of functionalization (8 nm, 2.5% DETA) were preferred.

Another relevant contribution to the understanding of the loading of MSNs pores with nucleic acids was reported by Li, Zhang and Gu, who studied DNA loading into small mesopores. In their studies there were employed 70 ± 20 nm magnetic MSNs with wormhole-like mesopores of 2–3 nm[105] and Dynamic Light Scattering (DLS) as a fast analysis technique to quickly differentiate the successful pore–DNA threading from the misplaced surface adsorptions. Finally, after finding an adequate chaotropic agent to balance the negative charges between DNA and MSNs, they achieved effective approximation and subsequent threading of DNA into mesopores. This strategy was applied soon afterwards to build MSNs as siRNA carriers for cancer therapy.[106]

The complete system was built with the 5′-(GCU ACU GCC AUC CAA UCG ATT)-3′ siRNAs as a pore filler, an outer protective layer of polyethyleneimine (PEI) and the KALA fusogenic

peptide (WEAKLAKALAKALAKHLAKALAKALKACEA) as a targeting moiety. The later grafting, achieved through the bifunctional linker (succinimidyl 3-(2-pyridyldithio)propionate) SPDP, produced a highly stable coating by bonding the terminal –SH cysteine moiety with the PEI coating. The *in vitro*/*in vivo* results showed an enhanced uptake onto the A549 alveolar adenocarcinoma human basal epithelial cells due to the targeting effect of the KALA peptide and an inhibited tumour growth due to the siRNA effect, thus validating the potential of the MSNs-based oligonucleotide gene therapy.

All these contributions were mostly aimed at the basic understanding of the loading and release processes. However, after the pioneering work by Qin *et al.* there was established a new niche of research in which these LP-MSNs carriers could be used to load, deliver and preserve nucleic acids from degradation inside living organisms. Following this premise, the group of Min compared the loading and release behaviour of both MSNs (2.1 nm) and LP-MSNs (23 nm) functionalized with amino groups.[107,108] They suggested that large-pore particles were able to host nucleic acids into their structure while regular-pore MSNs could only adsorb them at the surface. To demonstrate this, the authors loaded the corresponding nanoparticles with either the GFP plasmid DNA[107] or its opposite the GFP siRNA[108] and submitted both materials to a nuclease enzymatic assay prior to an *in vitro* testing. The authors only detected GFP transfection when loaded LP-MSNs were employed. This demonstrated the impossibility of loading the plasmid into the regular mesopores, as it was not preserved from degradation. In a complementary experiment using the GFP siRNA, parallel results were obtained; only siRNA@LP-MSNs were able to exert gene knockdown after the nuclease treatment, which validated their initial supposition.

Although the loading of plasmids/siRNAs might generate new materials for transfection technology, the truth is that up to now, all the reported systems showed an uncontrolled release. However, the previous experience in MSNs as drug delivery platforms could be quickly translated into those large pore materials to develop nanocarriers able to combine the protective role of pore entrapment with a pH-dependent release. Hence, in a nice approach for siRNA delivery by Hartono *et al.*, cubic LP-MSNs materials with pore sizes around 13.4 nm were functionalized with a biocompatible polylysine peptide.[109] As expected, the magnitude of the polypeptide chain showed a double and divergent behaviour, because DNA adsorption and toxicity by membrane destabilization were increased directly with the number of positive charges. The chosen siRNA sequences PLK (sense) 5′-(CCA UUA ACG AGC UGC UUA ATT)-3′; PLK (antisense) 5′-(UUA AGC AGC UCG UUA AUG GTT)-3′; Mirk (sense) 5′-(GGC ACU UCA UGU UCC GGA ATT)-3′; Mirk (antisense) 5′-(UUC CGG AAC AUG AAG UGC CGC)-3′, S10 (sense) 5′-(GCA ACA GUU ACU GCG ACG UUU)-3′; and S10 (antisense) 5′-(ACG UCG CAG UAA CUG UUG CUU)-3′ were successfully adsorbed onto the polylysine functionalized LP-MSNs. The viability tests performed on differently prepared siRNAs@MSNs against the osteosarcoma KHOS cancer cell line showed a reduction in viability due to an effective transfection of siRNAs.

As outlined previously, the development of enlarged porous silica nanomaterials has set the basis for development of materials able to carry nucleic acids with applicability in gene-therapy and transfection. Nevertheless, those examples mainly focused on the validation of the general process and not much attention has been paid to the material's nature. On this topic, Shi and co-workers reported the preparation of MSNs with different morphologies (hexagonal, cubic, lamellar and flower-like) but with common 12 nm size mesopores for transfection purposes,[110] although they made only the *in vitro* evaluation with the GFP plasmid and VEFG siRNA only with the spherical particles, completely bypassing the comparison between the different morphologies. Fortunately, contributions from other research groups have reported the use of other structures for this application. For example, in contrast to conventional LP-MSNs, the fibrous, dendritic KCC1 MSNs reported by Asefa and co-workers showed conical and broader pores than usual cylindrical materials.[111] This unique structure, although still untested, could also be a promising candidate with an upgraded loading capacity. Another example, reported by Meka *et al.*, employed cubic KIT-6 type MSNs with 9 nm pores for the delivery of Survivin siRNA.[112] Their results showed effective gene silencing, similar to those obtained using the commercial oligofectamine. The *in vitro* transfection of Survivin siRNA onto HCT116 colorectal carcinoma cells showed a dose-dependent cell inhibition of up to 40% for both 50 and 100 nM siRNA.

One of the fundamental governing mechanisms for the loading and delivery of nucleotides with MSNs is the electrostatic interaction between both counterparts, and particularly the electrostatic strength between the negatively charged NAs and the internal surface of pores. Indeed, the presence of opposite charges favours the hosting process but it may not be enough to avoid burst-type releases. To avoid this inconvenience several research groups have also contributed to the state-of-the-art with interesting approaches for pore gated systems. In a pioneering contribution, Rosenholm and co-workers designed LP-MSNs (3.5–5.7 nm) able to load short oligonucleotides whose premature release was avoided by a nanogate based on disulphide cleavable bond PEG units.[113] The bonding at the outermost surface of nanoparticles of these PEG chains was enough to avoid the nucleotide release due to the bulkiness of both elements. On this model the release was triggered by glutathione, which was able to cleave the disulphide bonds, thus detaching the bulky PEG moiety and allowing the release of the loaded nucleotide. In another contribution to this topic, Bein and co-workers designed a multifunctional polymeric shell for the delivery of therapeutic siRNAs employing 10 nm LP-MSNs (10 nm) or 5 nm-pored MSNs. In this model, there were designed materials with a positive pore surface able to drive the siRNA into the void pores.[114] This device was completed with disulphide cleavable bonds linked to a carefully tailored peptide block that was cross-linked through conveniently placed cysteine moieties.

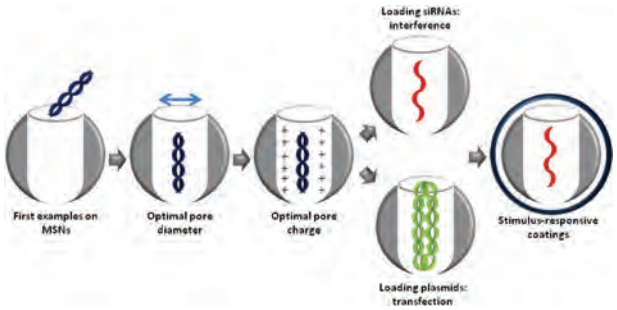

Fig. 8 Milestones achieved in the development of carriers for nucleic acids using MSNs.

This resulted in a redox-sensitive, cationic and disintegrable coating layer able to efficiently confine the GFP-luciferase siRNA. *In vitro* studies with this material showed effective fluorescence knockdown after 48 h on green stained KB cells, which demonstrated both the coating disintegration and the siRNA release (Fig. 8).

Another relevant approach for siRNA delivery with LP-MSNs, reported by Brinker and co-workers, employed supported lipid bilayers as MSNs' coatings (protocells). These systems, built from MSNs with pores in the range of 20–30 nm, were soaked in a siRNA solution to produce pore loading, which was further closed with the lipid bilayer.[115] During the coating process, which was achieved upon a gentle incubation of the siRNA-MSNs with cationic DOTAP liposomes, could be also included different but useful components. In this case two different targeting (SP94) and endosomolytic (H5WYG) peptides were incorporated into the phospholipid component by using a PEG-containing bifunctional linker. The loaded protocells were able to retain effectively the loaded siRNA and preserve it from nuclease degradation unless triggered by acidic media. These SP94/H5WYG-targeted, siRNA loaded protocells showed good stability and internalization, which resulted in exceptionally low IC90 values against the Hep3B cancer cell line with practically no adverse effects on normal hepatocytes (Fig. 8).

The promising interference efficiency achieved by LP-MSNs able to load siRNAs and the later design of protective multifunctional coating layers is still in its infancy and soon it could provide interesting contributions as a consequence of the incorporation of the improved aptamer mediated targeting. For example, an aptamer-targeted liposome for siRNA delivery has been reported with great performance.[116]

4.2 Surface deposition of nucleic acids onto MSNs for gene transfection and gene interference therapy

As reviewed, the possibility of loading nucleotides onto the promising LP-MSNs has also given access to deliveries able to avoid cargo degradation. However, most of the examples related with transfection and gene silencing are based on the surface deposition of oligonucleotide siRNAs and plasmids through electrostatic interactions.[117,118] This strategy, although it does not ensure an outstanding preservation, is highly versatile and suitable for these purposes. For instance, there have been reported successful nonviral siRNA deliveries with other systems like polymers,[119,120] peptides,[121] dendrimers,[122] lipids,[123] or metallic nanoparticles,[124] among many other systems.[125,126] In fact, the use of hybrid carriers containing polycationic fragments also enables the combination of features from both components. Among all the reported nanodevices, there could be highlighted those which facilitate endosomal escape,[127,128] or are able to perform a dual therapeutic action.[129,130]

The use of nanoparticles as a nonviral vector emerged as an attempt to develop a solution to the problem of toxicity in transfection technology, which is mostly based on the use of polycationic agents that induce cytotoxicity due to membrane destabilization. The first MSNs-based nonviral transfection example for mammalian cells was designed to avoid the use of common toxic cationic species like the already reported big, expensive and toxic high generation poly(amidoaminoamine) (PAMAM) dendrimers. For this, Lin and co-workers preferred the use of smaller sized dendrimers conveniently placed onto the particle's surface. So, their MCM-41 type particles loaded with Texas Red dye capped with a small 2nd generation PAMAM were able to exert a double function, producing pore capping while an adequate environment for DNA adsorption was generated.[131] Moreover, electrostatic deposition of the GFP plasmid onto this device proved to have an additional protective effect, as the DNA was not fully degraded in the presence of the BamHI endonuclease. In another contribution to the topic, MSN based devices were designed for gene transfection in plant cells, although in this case AuNPs were incorporated into the structure. These gold particles had a double task: first, they were included to increment the overall system mass in order to achieve the necessary kinetic energy to pass through the cellular wall when bombarded onto vegetal cells; and second, AuNPs helped in preventing uncontrolled leakage of the loaded compounds.[132] Moreover, this device was also able to adsorb plasmid DNA, like the model GFP plasmid, which upon bombardment produced effective transfection. This successful strategy was later adapted to build gold-plated MSNs of about 600 nm in which the 10 nm pores were able to load proteins. The gold plating improved projectile performance and allowed the transfection of different compounds such as GFP (28 kDa) or bovine serum albumin (66.8 kDa) as model proteins. Moreover, it was also possible to perform a combined delivery of both a Cre recombinase enzyme plus a chromosomal DNA to vegetal cells with a single device.[133,134]

Soon after the publication of those pioneer studies, other research groups started to make contributions which aimed at the simplification of the transfection systems based on MSNs. Interesting contributions were made by Gemeinhart and co-workers, who studied the transfection, the effect of surface charge of MSNs and their later destination in cells.[135] Moreover, Solberg and Landry studied the effect of cations with respect to the binding efficiency. They found that cations were able to balance the repulsive effect between DNA and

MSNs and for this purpose Mg^{+2} was particularly effective in comparison with other ions such as Na^{+} or Ca^{+2} because of a better balance generated by a stronger interaction with the phosphate groups present in nucleic acids.[136]

All those reviewed contributions helped in clarifying the governing mechanisms of adsorption–desorption between DNA and SiO_2, which are valid for both pore-loading and surface deposition strategies. Nevertheless, the truth is that these models are far away from the unbeatable performance of viruses in the delivery of genetic information, which may lead us to think that MSN based transfection technology is in a dead end.[137] Nevertheless, this technology has not fallen into oblivion as it has been extensively employed for the delivery of other nucleic acids with different effects: siRNAs[96,138] and for the development of novel combination therapies based on the simultaneous effect of carried drugs and siRNAs.

The large surface area of MSNs in comparison with the relatively small size of siRNAs provides enough binding space for multiple strand loading and thus increased efficiency, although in this case, siRNAs demand more space as they should be deposited through electrostatic interactions or cleavable bonds, as their therapeutic effect relies on a final siRNAs release. One of the first contributions to the topic was reported by Cho and co-workers, who developed mannose-targeted polyethyleneimine-coated MSNs for the delivery of nucleic acids. In their model, the PEI had a double purpose surface modification: to provide a positive coating for DNA deposition and to enable effective transfection due to the detachment and endosomal escape of DNA through the so-called 'proton sponge effect' (Fig. 9).[139] This device showed an improvement in cell viability of both Raw 264.7 and HeLa cell lines in comparison with the high molecular weight PEI. After the pioneering use of PEI coating, more recently Nel and co-workers studied the effect of the molecular weight of PEI onto MSNs towards gene silencing applications. In their studies they found that high molecular weight PEI, even when employed as a coating, increased cellular death due to the polymer cytotoxicity. On the other side, the lower weight polymers did not show this toxic effect although they were not able to bind so efficiently the corresponding siRNA. Then with the optimal medium-weight PEI coating they tested the performance of MSNs loaded with the GFP siRNA; their results showed successful silencing of cellular fluorescence on HEPA-1 liver cancer cells without significant cytotoxicity.[140]

This PEI coating was also studied by Coradin and co-workers from another point of view; they focused their efforts on understanding the effects of MSN substitution patterns prior to the PEI deposition.[141] They found an interesting behaviour related to the particle functionalization, which after PEI coating showed lower nucleotide loading efficiencies in the case of strong anionic substituted MSNs. On the other hand, according to their results, slightly anionic PEI-coated MSNs had a better loading profile. More recently and along this line, Lellouche and co-workers implemented a process to coat MSNs with high molecular weight PEI which avoided the cytotoxic effect of such polymers. In their contribution, the authors employed nontoxic Ce^{+3} cations[142] to produce PEI grafting onto the silica surface; this strong cross linkage of PEI generated a significant decrease of the system toxicity due to its retention onto the nanodevice. Their studies with anti-GFP sense 5′-(GGA CAU CAC CUA UGC CGA GUA CUT C)-3′ and anti-GFP antisense 5′-(CAC CUG UAG UGG AUA CGG CUC AUG AAG)-3′ siRNAs demonstrated an effective down-expression of luciferase in U2OS-Luciferase modified cells without compromising viability. Another interesting possibility to avoid the toxic effect of high molecular weight PEI was reported by Yu *et al.*, who employed epoxy-functionalized ultra-small MSNs (USMSN, about 10 nm) to achieve permanent grafting of PEI to the surface.[143] These small particles proved to be easily taken up upon electrostatic complexation of the negatively charged siRNAs, and when tested against polo-like kinase 1 (PLK1-siRNA) for osteosarcoma cancer cells (KHOS) and Survivin-siRNA for human colon cancer cells (HCT-116) they showed a significant cell growth inhibition comparable to that obtained with the commercial oligofectamine.

The MSN@PEI@oligonucleotide multilayer deposition (Fig. 9) strategy has also been used for the construction of targeted, gene silencing nanodevices employing the sense: 5′-(CAC GUU UGA GUC CAU GCC CAA UU)-3′ and antisense: 5′-(UUG GGC AUG GAC UCA AAC GUG UU)-3′ HER2-siRNAs. In this model, reported by Ngamcherdtrakul *et al.*, a MSN core was coated with PEI to enable HER2-siRNA deposition. Additionally, in this device the PEI layer was further tailored with Trastuzumab antibody through PEG chains, thus achieving a double protective and stealthy effect due to the PEG chains and active delivery against HER2 positive breast cancer cells thanks to the antibody targeting.[144] The authors demonstrated *in vitro* and *in vivo* that the system thus designed was successfully taken up by HER2 positive cells, in which was produced the expected gene silencing and the restoration of drug sensitivity. Furthermore, this siRNA delivery induced apoptotic death of HER2 positive cells, while the negative cells remained unaffected, opening the door to the construction of synergistic therapy nanodevices (section 4.3). In another interesting contribution by Wu *et al.* the authors demonstrated the potential of Large-Pore ultrasmall mesoporous organosilica nanoparticles (LP-us-MONs) for transfection purposes.[145] Onto this system, with pores large enough to accommodate nucleotide macromolecules, the authors grafted successfully PEI polymers further decorated with the cell-penetrating TAT peptide. These nanodevices were able to successfully enter first the cell and later migrate to the nucleus, efficiently transfecting the GFP

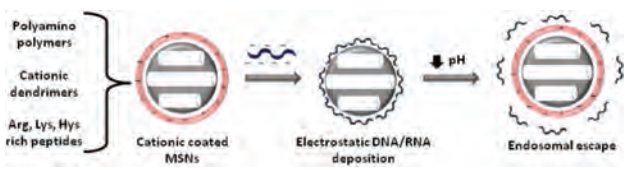

Fig. 9 Electrostatic deposition of NAs onto MSNs. Strategies for gene delivery and silencing.

plasmid, upon reduction of a dithiol bond responsible for bridging the PEI polymer to the LP-us-MONs.

Apart from polyamine polymers, which have been profusely employed for the construction of siRNAs as delivery devices, there is another family of polymeric materials able to perform this task: cationic peptides, which could act also as nucleotide carriers if properly functionalized.[121] The main advantages of cationic oligopeptides in comparison with polymeric compounds are: a well-established custom synthesis, the possibility of obtaining narrow weight distributions, the tailorable size and composition and, mainly, their biogenic origin. This not only provides outstanding biocompatibility but also may contribute additional features typical of proteins: recognition, signalling or even catalytic activity.[146] Because of this, there is an increased interest in the development of peptide-based nanosystems able to exert combined biological effects in combination with siRNAs (Fig. 9).

Among all known peptides, the most recurrent examples for gene delivery purposes are polylysine[109] and the KALA fusogenic peptide.[106] Nevertheless, there have been also designed other interesting peptides able to efficiently interact with siRNAs. In an interesting contribution, Lu *et al.* designed a double role peptide chain in which an 8 unit polylysine region was responsible for the non-covalent binding to oligonucleotides and other sequences (KSLSRHDHIHHH) with preferential interaction towards silica thanks to a multiple ion pairing.[147] The binding abilities of the KSLSRHDHIHHHKKKKKKKK peptide permitted effectively bridging both LP-MSNs and the CpG oligodeoxynucelotide 5′-(TCC ATG ACG TTC CTG ACG TT)-3′. The *in vitro* results with this nanohybrid demonstrated competitive interference of the miR29b mRNA and then collagen production knockout rates similar to those obtained with the commercial lipofectamine.

The huge toxicity reduction achieved when cationic moieties are irreversibly grafted onto MSNs opened the door for the incorporation of highly charged polymeric materials, such as high molecular weight PEIs, which are able to load greater amounts of nucleic acids. However, the real advantage of the grafting strategy relies on the possibility of fine tuning the surface charges. For example, in a contribution by Vallet-Regí and co-workers, the functionalization of MSNs with carbosilane dendrimeric branches allowed grafting a perfectly known number of permanent cations.[148] For this study, the authors took advantage of the high molecular weight of the dendrimeric branches, which allowed the precise estimation of branches incorporated through systematic thermogravimetric measures; furthermore their narrow weight distribution allowed the development of an unprecedented hybrid material with great possibilities for transfection and gene therapy (Fig. 9).

Another novel application reported of peptide functionalized MSNs, although outside the scope of the present review, is the size separation of DNA fragments,[149] which relies on the variable electrostatic interaction between DNA strands and polylysine chains. In both cases, DNA and polylysine, the number of charges is directly correlated with the chain length, so the maximal electrostatic interaction would only occur when all charges (electrostatic repulsions) are balanced. So, the interaction of a fixed-length polylysine string with different length DNA strands would be maximal only for the length able to balance all charges, leading to an electrostatic matching (length-based) separation of nucleotides. The potential of this strategy for oligonucleotide deliveries is enormous, as it may bypass any eventual displacement of the loaded nucleotide by any other species present.

Oligonucleotide transfection technology employing MSN based devices has opened the door to the development of multifunctional delivery agents with relatively low toxicities and good efficiencies. Nevertheless, between the two strategies, it is difficult to distinguish which one would provide better results for extensive applications. On the one hand, the in-pore loading of oligonucleotides claims an outstanding preservation of the loaded DNA exclusively for porous materials; however, the complexity and uncertainty of the loading process make this transfection a risky process for extensive applications. On the other hand, the surface deposition of DNA/RNA being a very simple, controllable and measurable process allows a better control over the loading and thus the development of multi-compound delivery, of great interest for drug combination purposes. In summary, although DNA pore loading could be of interest due to nucleotide preservation (please refer to section 5.4), the versatility of surface deposition is undoubtedly of greater interest for biomedical applications, as would be reviewed in the following section.

4.3 Combination of chemotherapeutic delivery with gene therapy using MSN based carriers

The bigger pore size of LP-MSNs allows the loading of nucleic acids and opens the door for the development of a new family of biomacromolecular carriers. Nevertheless, the main efforts are still focused on the use of MSNs as platforms for small molecule delivery, like sensing probes (section 5) or antiproliferative compounds, which are expected to upgrade the current cancer therapy. Indeed, as the role of nucleic acids is the maintenance, transcription and expression of genetic information within the cell, they are necessary participants in the development of future gene therapies against cancer. Notwithstanding, nanocarrier technology is developed enough to build systems able to simultaneously deliver cytotoxic and gene expression modulators, which promise to reduce the severe side-effects of common chemotherapy while gene therapy is also exerted.[130,150,151]

As will be reviewed, the delivery of multiple therapeutic species with a single device shares some of the ideas developed for gated systems. Hence, as the incorporation of therapeutic nucleic acids onto MSNs is mostly based on the electrostatic multilayer deposition of NAs onto MSNs, there could be foreseen a parallel development for the systems that combine cytotoxic delivery plus gene modulation. Some of the advantages of this well established methodology are the possibility of preparation through a simple methodology, the resulting

prevention of drug leakage due to the outer layer and finally a proton-sponge driven release that only operates in intracellular (lysosome/endosome) environments.[127,128] Another crucial aspect to obtain a significant therapeutic behaviour is the adequate selection of both siRNAs and cytotoxics. From all the reported antiproliferative compounds, doxorubicin is of preference as it shows an enhanced release at low pH values. On the other side, siRNAs able to block the common drug-resistance routes are the most exploited as they maximize the therapeutic effect of most of the cytotoxics. Among all known surviving mechanisms which have been the object of siRNA modulation, ATP-dependent drug-efflux pump membrane proteins such as *p*-glycoprotein (Pgp),[152,153] B-cell lymphoma 2 protein family (Bcl-2)[154,155] and heat-shock proteins[156] as apoptosis inhibitors are the most recurrent examples when referring to MSNs.

In the first contribution aimed at cancer treatment, Chen *et al.* employed the developed transfection strategy which used a 2nd generation PAMAM dendrimer to deliver the Bcl-2 anti-apoptotic siRNA, although in this case DOX was loaded into the mesopores.[157] The combined effect of both agents showed a 132-fold increased apoptosis in comparison with free DOX, obtained by the suppression of the Bcl-2 mediated resistance in A2780/AD human ovarian cancer cells (Entry 1, Table 2). Employing a similar strategy Zhao *et al.* reported a design which employed PEI as a linking material between MSNs and siRNA; moreover, in this case folic acid was incorporated as an active targeting molecule.[158] Again, the evaluation of this device against the folate-positive (HeLa) cell line showed reduced cell viability due to the disruption of Bcl-2 protein expression. Furthermore the presence of folate increased the internalization rate through active targeting[10] (entry 2, Table 2). The same cationic bridging polymer PEI was employed by Meng *et al.* for the delivery of DOX and Pgp siRNA combinations with pH-dependent release.[159,160] As expected, in both examples the down-expression of Pgp disrupted the drug-efflux effect and produced local increases of drug concentration which enhanced cellular death. It is also noteworthy that for this model the authors did a systematic

Table 2 Models for chemo- plus interference gene therapy based on MSNs

Entry	Delivery system[a]	siRNA[b]	Linking material[c]	Targeting cargo[d]	Cell line	Ref.
1	MSNs	Bcl-2 S: 5′-(GUGAAGUCAACAUGCCUGCdTdT)-3′ AS: 5′-(GCAGGCAUGUUGACUUCACdTdT)-3′	G2 PAMAM	None/DOX	A2780/AD (ovarian)	157
2	Hollow MSNs	Bcl-2 S: 5′-(rGrUrArCrArUrCrCrArUrUrArUrArArGrCrUGrUrCrGrCdAdG)-3′ AS: 5′-(rUrGrCrGrArCrArGrCrUrUrArUrArUrArArUrGrGrArUrGrUrArCrUrU)-3′	PEI	Folate/DOX	HeLa, MCF-7 (breast)	158
3	MSNs	Pgp S: 5′-(r(CGGAAGGCCUAAUGCCGAA)dTdT)-3′ AS: 5′-(r(UUCGGCAUUAGGCCUUCCG)dTdG)-3′	PEI	None/DOX	KB-31, KB-V1 (cervix)	159
4	MSNs	Pgp: 5′-(CGGAAGGCCUAAUGCCGAAtt)-3′ MRP1: sc-35962* ABCG2: sc-41151* Bcl-2 5′-(GUGAAGUCAACAUGCCUGCTT)-3′ cMYC: sc-29226* PXR: sc-44057*	PEI	None/DOX	MCF-7 (breast)	160
5	LP-us-MONs	Pgp	PEI	None/DOX	MCF-7 (breast)	161
6	MSNs	anti-luciferase anti-GAPDH	PDMAEA	None/CLQ	B16F10 (murine melanoma)	162
7	LP-MSNs	PLK-S: 5′-(CCAUUAACGAGCUG CUUAATT)-3′ PLK-AS: 5′-(UUAAGCAGCUCGUUAAUGGTT)-3′ S10-S: 5′-(GCAACAGUUACUGCGACGUUU)-3′ S10-AS: 5′-(ACGUCGCAGUAACUGUUGCUU)-3′	PDMAEA	None/CLQ	KHOS (bone)	163
8	MSNs	Anti-miR221 $(Arg)_8$-5′-(GCAGACAATGTAGCT)-3′Gly-NH_2	Peptide-NA hybrid	None/TMZ	C6, T98G (glioma)	164
9	MSNs	VEGF S: 5′-(GGAGUACCCUGAUGAGAUC)-3′ AS: 5′-(GAUCUCAUCAGGGUACUCC)-3′	TAT/PAH-Cit/GTC Multilayer	TAT/DOX	QGY-7703 (hepatic)	165
10	Magnetic MSNs	Vasohibin-2 (VEGF) S: 5′-(GGAGUACCCUGAUGAGAUCdTdT)-3′ AS: 5′-(GAUCUCAUCAGGGUACUCCdTdT)-3′	PEI	KALA/None	SKOV3 (ovarian)	166
11	AuNR@MSNs	S: 5′-(HS-$(CH_2)_6$-GCAGCACGACUUCUUCAAGTT)-3′ AS: 5′-(CUUGAAGAAGUCGUGCUGCTT)-3′	cRNA	None/DOX		167

Abbreviations: [a]AuNR, gold nanorods; [b]S, sense siRNA; SA, antisense siRNA; Pgp, *p*-glycoprotein; Bcl-2, B-cell lymphoma 2 family; PLK, polo-like kinase; VEFG, vascular endothelial growth factor; GAPDH, glyceraldehyde 3-phosphate dehydrogenase; *Commercial siRNAs from Santa Cruz Biotechnology (Santa Cruz, CA); [c]PAMAM, poly(amidoaminoamine) dendrimer; PEI, poly(ethyleneimine); PDMAEA, poly(2-dimethylaminoethyl-acrylate); cRNA, complementary siRNA oligonucleotide; [d]DOX, doxorubicin; CLQ, chloroquine, TMZ, temozolomide; TAT, transactivator of transcription peptide (YGRKKRRQRRR).

evaluation of several pump dependent (Pgp, MRP1 and ABCG2) and non-pump dependent (Bcl-2, cMyc and PXR) proteins. They found that the DOX–Pgp siRNA combination showed the best therapeutic effect due to drug resistance reversion (entries 3 and 4, Table 2). This DOX–Pgp siRNA has also been successfully employed with large-pore ultrasmall organosilica nanoparticles previously reported by Wu *et al.*,[145] although in this case the previously used TAT penetrating peptide was not employed[161] (entry 5, Table 2). Again, this device was built to enhance its response to intracellular reducing media, due to the presence of cleavable dithiol bonds between the LP-us-MONs and the polymeric PEI coating responsible for siRNA adhesion.

In another interesting contribution to the topic, Bhattarai *et al.* first and Hartono *et al.* later developed and tested a disintegrable cationic polymeric layer based on poly(2-dimethylaminoethylacrylate) for MSNs coating. This polymer, known to hydrolyse under smooth physiological conditions, released the cationic 2-dimethylaminoethanol fragment when subjected to a lysosomal environment. This produced a disassembly of the cationic surface that allowed the effective release of the therapeutic nucleotide. In the first model, by Bhattarai *et al.*, after validation with the anti-luciferase siRNA, the authors employed the glyceraldehyde 3-phosphate dehydrogenase (GADPH) siRNA able to arrest glycolysis, which in combination with CLQ reduced significantly the cell viability[162] (entry 6, Table 2). In the later example, the authors improved the grafting step of the polymer through a click-process. Again, as expected, they obtained a similar behaviour with enhanced antiproliferative effect against the KHOS cell line with combinations of CLQ and PLK or S10 siRNAs (entry 7, Table 2).[163]

Apart from intracellular Bcl-2 or ABC-transporters (such as Pgp) siRNAs, there have been also reported interference therapies on angiogenesis. This, aimed to produce nutrient outage on the tumour areas, is also an interesting approach for future combination therapies. Along this line, De Cola's group reported the disruption of microRNA 221 (miR221), involved in angiogenesis, to reverse drug resistance of Temozolomide (TMZ) in resistant gliomas.[164] In this design there was included a significant innovation as there was suppressed the polymeric linking material; instead, the authors bound a cationic peptide sequence to the oligonucleotide to generate a peptide–siRNA hybrid capable of being directly adsorbed onto the silica. *In vitro* studies on T98G glioma cells with this system proved again that simultaneous therapy shows a better profile than separated therapies (entry 8, Table 2).

In another co-delivery involving antiangiogenic interference, Yin *et al.* reported the combination of a Vascular Endothelial Growth Factor (VEGF) siRNA, able to produce nutrient outage at the tumour area, a cytotoxic payload and a cell penetrating peptide as a cellular targeting molecule.[165] In this device the authors designed a complex polyelectrolyte multilayer, which was built up as follows: first, the DOX loaded MSNs were functionalized with the cationic TAT peptide and then a negative poly(allylamine hydrochloride)-citraconic anhydride (PAH-Cit) layer was deposited onto those TAT-MSNs. Finally a galactose-modified trimethyl chitosan–cysteine (GTC) conjugate occupied the outermost layer to bind clathrin heavy chain-1 (CHC-1), caveolin-1 or Rac1 siRNAs. The evaluation of this system against human hepatocarcinoma provided good results in arresting proliferation of cancerous cells as no additional guidance was required to reach the liver (entry 9, Table 2). The huge potential effect of anti-VEFG siRNAs was also employed by other authors with promising results. In a contribution by Chen *et al.* the authors employed a different inhibitor, Vasohibin-2 siRNA, to build a device based on KALA fusogenic peptide targeted magnetic MSNs. Although in this model an antiproliferative drug was not employed, the combined action of siRNA plus the effect of KALA peptide proved to be effective for the *in vivo* treatment of ovarian adenocarcinoma tumors[166] (entry 10, Table 2).

As reviewed, MSNs can be employed to obtain highly promising nanodevices able to exert more than one apoptotic effect. Nevertheless, this could be even implemented by adding some of the additional features reported for MSN hybrids. Along this line, in a visionary work by Yeh and co-workers, there was employed gold nanorods (AuNR) with silica coating (AuNR@MSNs) onto which was incorporated a siRNA-based nanogate[167] (entry 11, Table 2). The authors thus created a near-infrared (NIR) responsive system able to perform a controlled dual release of the hosted cytotoxic DOX together with the gate keeper siRNA. Contrary to other reviewed systems, in this case release is not endogenous but dependent on an external stimulus, which by the way is able to induce a third apoptotic mechanism (hyperthermia/photoablation). Unfortunately, this model was poorly developed as only independent experiments of drug-delivery and GFP down-expression were performed; nevertheless future investigations of this device might lead to outstanding therapeutic profiles.

5. Sensing and detection nanodevices based on DNA–silica hybrids

The outstanding sensitivity and specificity of DNA based recognition has gained attention for the development of a great number of sensors. Of all the reported sensors, nanobeacons,[168] extensively employed for the specific detection of low amounts of DNA strands, are one of the most successful approaches. Nanobeacon sensing technology relies on the known conformational shifts of DNA strands when properly paired with a complementary strand. Moreover, it also depends on the effective fluorescence quenching between a fluorophore and a quencher. Briefly, the working mechanism for those devices is based on the three dimensional conformational change suffered by the sensing DNA strand in the presence or absence of its base-matching complementary sequence. For example, a system designed to put close in space both photoactive species when dehybridized will show

no fluorescence, unless in the presence of the complementary strand, which would produce DNA hybridization and separation of both the fluorophore and the quencher. This technology, mostly based on AuNPs[169–171] due to their known quenching effect, has a broad impact in cellular biology as it allows the *in vitro*/*in vivo* detection of particular DNA strands. But the extraordinary recognition ability of DNA makes these systems suitable for the detection of other non-nucleotide motifs like macromolecules, small molecules or even certain cations in the case of DNAzymes. For example, parallel designs employing aptamers have been used to detect proteins[172] or small molecules.[173]

Although nanobeacon and aptasensing technology based on AuNPs is well established, there are still important drawbacks that limit a possible all-purpose utilization. For example, a common limitation is that AuNPs tend to aggregate if they are either not properly stabilized by the DNA[174] or they are in high ionic strength media. Although this may be interesting for colorimetric detection of gold, it may also lead to premature failures of those devices. Another important drawback is the lower detection limit of fluorophores, which are usually set to one per DNA strand. All these issues, added to the low loading degree of AuNPs, may disfavour the detection process due to an overall poor response. Fortunately the use of MSNs, with greater loading capacity and lower self-aggregation rates, could provide interesting platforms for the construction of DNA-based sensors with improved detection limits. Although most of the reported MSN-based sensors are based on immobilization of either enzymes for colorimetric detection[175,176] or catalyst integration,[177,178] there are also interesting examples in which DNA is employed as the sensitive moiety. For a comprehensive and recent review dealing with MSNs in sensing applications please see ref. 24.

5.1 Detection of macromolecules

In previous examples we have focused our attention on aptamer mediated guidance. However, the role of aptamer–MSNs hybrids is not only restricted to vectorization, as aptamers can be also employed for the construction of molecular gates and thus the detection of biomacromolecules. In those cases, if the substrate is able to generate a conformational change, the pores would be opened and, if properly loaded, induce the release of measurable compounds. For example, Ren *et al.* reported a proof of concept in which the electrochemically detectable methylene blue was employed to build a sensor able to detect DNA-labelled antibodies.[179] In this sensor the authors employed the short 5′-(GTA ATC CTC AGC AAC CTC AGC)-3′ strand to cap mesopores through electrostatic deposition. There were employed two partially complementary strands bound to two different antibodies as the release stimulus (DNA-Ab1: 5′-(GCT GAG GTT AT*C AAG AC*T TTT TTT ATC ACA TCA GGC TCT AGC GTA TGC TAT TG-SH)-3′-Ab; DNA-Ab2: Ab-5′-(SH-TAC GTC CAG AAC TTT ACC AAA CCA CAC CCT TTT TTT *GTC TTG* GCT GAG GAT)-3′). In order to facilitate recognition between the three involved counterparts, the authors employed strategic complementary sequences between both DNA-Ab hybrids to facilitate the antibodies' approach and thus an enhanced pore uncapping.

Another approach for the development of aptamer-based sensors is the use of electrochemical immunosensors, which offer high sensitivity, low cost and ease of miniaturization when compared to fluorescence, chemoluminescence or surface-plasmon resonance based sensors. On this topic, in a contribution by Yuan and co-workers, thrombin was chosen as the substrate and the thrombin-binding aptamer (TBA) 5′-(GGT TGG TGT GGT TGG)-3′ was employed as the detector in a two-component amplifiable electrochemical aptasensor.[180] Briefly, in this example a graphene oxide electrode (GOe) and a MSN coated carbon nanotube (CNT@MSN) were functionalized with the same aptamer; which allowed the substrate thrombin to bridge both subunits through a sandwich like structure. The proximity of both units allowed an outstanding detection for the electrochemically active thionine released from the mesopores. Although this double component sensor is undoubtedly complex, it is remarkable that double aptamer binding to macromolecules is possible and may open up broad potential application for clinical assays in proteins, pathogens[181] and diseased cells;[57] which actually are the primary source of macromolecules.

As outlined in previous sections, DNA–MSNs hybrids for gene silencing therapy have been successfully employed for cancer treatment. Unfortunately, all the approaches designed offer no information on the degree of silencing or its efficiency. With this idea in mind, Liu and co-workers designed a MSN based sensor for the detection of the oncogenic miRNA-21. For this, they employed an adapted version of nanobeacons in which MSNs were functionalized with two different nucleic acids.[182] The first, the AS1411 aptamer, was responsible for targeting and internalization, while the second was a fluorescently labelled miRNA-21 complementary sequence, 5′-(H_2N-AA-S-S-TCA ACA TCA GTC TGA TAA GCT ATG TCG CTT-FAM)-3′ (MB_L). This latter MB_L strand was linked to MSNs through a dithiol-cleavable bond and hybridized with the complementary 5′-(Dabcyl-GCG ACA TAG CT)-3′ strand. This resulted in an effective fluorescence quenching of the FAM fluorophore at the MB_L strand with the Dabcyl quencher as its complementary strand. The action mechanism of the device included an AS1411 mediated uptake into MCF-7 cells; once internalized, the presence of the intracellular miRNA-21 displaced the MB_L from the dabcyl containing strand. This seizure of the mature mRNA and the reactivation of fluorescence produced a double effect: quantification of the oncogenic mRNA and a possible disruption of the oncogenic pathway. In another interesting contribution to the detection of biomacromolecules, Xu, Chen and co-workers developed a nanosensor responsive to the antiapoptotic Survivin mRNA. In this device the authors employed the multilayer electrostatic deposition to coat $Ru(bipy)_3^{+2}$ loaded amino-functionalized cationic MSNs with the survivin siRNA.[183] In this case the presence of the target mRNA produced the displacement of the siRNA at the biogate, allowing the release of the fluorescent traceable probe. In both examples the purpose for the devices

was only the detection of oncogenic/antiapoptotic mRNAs; however, they could be also employed as interesting platforms for the delivery of silencing-based therapeutics; unfortunately, no antiproliferative effect was studied, so both devices were only designed as proofs of concept.

The fluorescent detection of taken up particles has been extensively employed for the understanding of their metabolism and biodistribution in both *in vitro* and *in vivo* models. So fluorescent tagged particles[184] play an important role in the detection, although they also show disadvantages which reduce their application for quantification purposes. One of these is the so called aggregation-caused quenching (ACQ) effect, which is an intrinsic property of common fluorophores which lose their efficiency as the concentration increases. This effect limits enormously the response and thus the possible quantification of the tagged particles. Nevertheless, there is another kind of fluorescent material with the opposite effect: aggregation-induced emission (AIE) fluorophores, which are of great interest for tagging nanoparticles with detection and quantification purposes. Along this line, Wang *et al.* have reported the use of AIE fluorophores in the construction of nanomaterials with enhanced fluorescence, mainly when aimed at the detection and quantification of cells.[185] In their example, reported using AS1411 aptamer targeting, there was obtained a linear relationship between the number of internalized particles and fluorescence, which could be of interest for the detection of highly accumulated particles.

Although bright fluorescence imaging is the most recurrent strategy for the detection and quantification of nanoparticles, magnetic MSNs (mMSNs) have also enormous possibilities. Two of the most interesting features for detection are Magnetic Resonance Imaging (MRI) and sample enrichment through magnetic decantation and isolation. In a nice example, Deng and co-workers designed a nanodevice able to specifically isolate insulin hormone from biological fluids for improved detection. Their device was based on magnetic MSNs capped with AuNPs further decorated with the insulin-binding aptamer (IBA) 5′-(ACA GGG GTG TGG GGA CAG GGG TGT GGG G)-3′, which was able to attach insulin onto a magnetically isolable device.[186] This strategy allowed the collection and concentration of insulin from biological fluids due to the specificity of the aptamer, which allowed further analysis with increased sensitivity. The identification of bound compounds was carried out by MALDI mass spectrometry from the fraction obtained after thermal dissociation. In all tested cases, independently of the presence of other peptidic compounds, insulin was the only compound retained thanks to the great specificity of the aptamer–substrate interaction.

The extraordinary affinity of aptamer–substrate pairing has allowed the development of powerful nanosensors able to perform the specific recognition of biomacromolecules. However, as cells are the primary source of biomacromolecules, it would be also possible to develop sensors for cells and tissues. Some interesting examples following this idea were reported by (1) Xu and co-workers, who reported the use of a Gd-containing mMSNs nanoprobe targeted with the AS1411 aptamer for cellular detection of renal carcinomas;[187] (2) Zhao and co-workers, who reported the detection of leukaemia cells using solid silica nanoparticles targeted with the Sgc8 aptamer 5′-(H_2N-TTT TTT TTT TAT CTA ACT GCT GCG CCG CCG GGA AAA TAC TGT ACG GTT AGA)-3′;[188] and (3) Ban and co-workers, who reported the use of fluorescent solid SiO_2 nanoparticles targeted with MUC1 5′-(GGG AGA CAA GAA TAA ACG CTC AAG CAG TTG ATC CTT TGG ATA CCC TGG TTC GAC AGG AGG CTC ACA ACA GGC)-3′ and HER2 5′-(AAC CGC CCA AAT CCC TAA GAG TCT GCA CTT GTC ATT TTG TAT ATG TAT TTG GTT TTT GGC TCT CAC AGA CAC ACT ACA CAC GCA CA)-3′ aptamers for the specific recognition and detection of breast cancer cells.[189]

5.2 Detection of small molecules

Aside from the use of aptamer–MSNs hybrids for the detection of biomacromolecules, detection of other small molecules with responsive gated materials is also possible. The first reported models sensitive to discrete molecules were focused on the detection of ATP, which has been reviewed and classified in the precedent section 3.2 and extensively reviewed in ref. 24.

On this topic, there have been reported other examples in which the sensing task relies exclusively on DNA and the silica acts only as a convenient nanometre sized platform. In one of those examples, there was grafted to the silica the 5′-(H_2N-$(CH_2)_{12}$-ACC TTC CTC CGC AAT ACT CCC CCA GGT)-3′ (≈0.3 nmol mg^{-1}) anchor strand through amide bonds. This strand was further hybridized with the complementary 27-mer ATP aptamer 5′-(ACC TGG GGG AGT ATT GCG GAG GAA GGT)-3′, thus generating a functionalized dsDNA able to intercalate the Hoechst 33258 dye in between T-A pairings and able to be displaced by ATP molecules.[190] Thus, the presence of the triggering stimulus produced the release of an intercalated dye through seizure of the aptamer, which allowed the inverse fluorescence quantification of ATP. This nanosensor provided linear responses from 0 to 0.2 mM and detection limits of 20 μM with good selectivity towards ATP due to the specificity of the aptamer. A major drawback of this design is the huge amount of dye required; for this, Lu *et al.* designed an implementation in which the Cy5 fluorophore was directly bound to the aptamer strand. This modification allowed a substantial reduction (from 11 to 1) of the overall amount of fluorophore.[191] Moreover, if the employed SiO_2NPs are replaced by Ag@SiO_2, an increase on the Cy5 fluorescence occurs, which improves the neat efficiency of the system by maintaining sensitivity unaltered.

Although well developed, the quantification through subtracted fluorescence still presents development disadvantages due to the huge cost of fluorophores and linkers. In order to overcome this problem, Wu *et al.* reported the use of upconversion $NaYF_4$:Yb,Er@SiO_2 particles as fluorescent tags. Their model was based on the use of two different silica nanoparticles with different properties. On the one hand the authors prepared mMSNs to which they grafted the 5′-(H_2N-CGA CCG TGG GAC AAC TCA)-3′ anchor sequence, while on

the other hand there were prepared, through avidin–biotin bridging, chloramphenicol aptamer 5′-(Biotin-AGC AGC ACA GAG GTC AGA TGA CTT CAG TGA GTT GTC CCA CGG TCG GCG AGT CGG TGG TAG CCT ATG CGT GCT ACC GTG AA)-3′ functionalized upconversion nanoparticles. The combination of both MSNs and upconversion particles produced a magnetically decantable supramolecular construct sensitive to chloramphenicol,[192] a molecule that released the traceable upconversion particles.

The possibility of combining DNAs with MSNs has proved to be of great interest for the development of sensors. Indeed, the possibility of responding to more than one stimulus, that is, more than one macromolecule, is also possible and has been explored by Ren, Qu and coworkers in an elegant model. For this, the authors designed a mesoporous material to which were appended successively different DNA strands which could be only opened when the adequate complementary strands are present and are in a correct order.[193] For this, MSNs were functionalized through an amide bond to the "D"-sequence, which was bound to sequence "C" that is able to bridge both "D" and "B" sequences. Iteratively, the "B" strand could further hybridize both "C" and "A" sequences, thus giving multi-hybridised cascades, which are only released when the complementary sequences A′, B′ and C′ are employed (A: 5′-(GAA GAC TCG TAA TGT GAA ACC G)-3′; B: 5′-(CAC ATT ACG AGT CTT CGT GGC ATA TCA CTC TTG GAG)-3′; C: 5′-(GGG GTC CGC TAT AAA CAC CTC CAA GAG TGA TAT GCC AC)-3′; D: 5′-(GTG TTT ATA GCG GAC CCC)-NH_2-3′).

5.3 Detection of pollutant cations

As outlined previously, one of the main advantages of nanosensors based on DNA–MSNs hybrids is the possibility of non-linear response against external stimuli. This is of special interest in the detection pollutant cations, which usually are present on trace quantities. Some of the already reviewed examples employ cation dependent DNAzymes or G-quadruplexes to build nanogates onto MSNs. So the need for those cations to induce cargo release (section 2) could be considered cation detection too. However, those examples are limited to common or low pollutant elements such as K, Mg, Zn, *etc*. with the only exception of UO_2^{+2}.

In an effort to extrapolate this detection technology to other cations, two independent research groups reported the use of DNAzyme–MSNs hybrid sensors for the detection of Pb^{+2}. In the contribution by Tang and co-workers the detection relied on the Pb^{2+}-sensitive DNAzyme strand 5′-(TTT CAT CTC TTC TCC GAG CCG GTC GAA ATA GTG AGT)-3′, which could block the pore after hybridization with the 5′-(ACT CAC TAT *r*AGG AAG AGA TG)-3′ anchor strand grafted onto MSNs.[194] Contrary to other examples in which detection relied on fluorophores, glucose was chosen as it allowed detection with commercial portable glucometers (Fig. 10). More recently, Yang and co-workers reported a similar strategy in which the cleavable strand 5′-(H_2N-ACT CAC TAT *r*AGG AAG AGA TG)-3′ and the Pb^{+2} dependent DNAzyme–biotin hybrid 5′-(CAT CTC TTC TCC GAG CCG GTC GAA ATA GTG AGTA-biotin)-3′ were hybridized

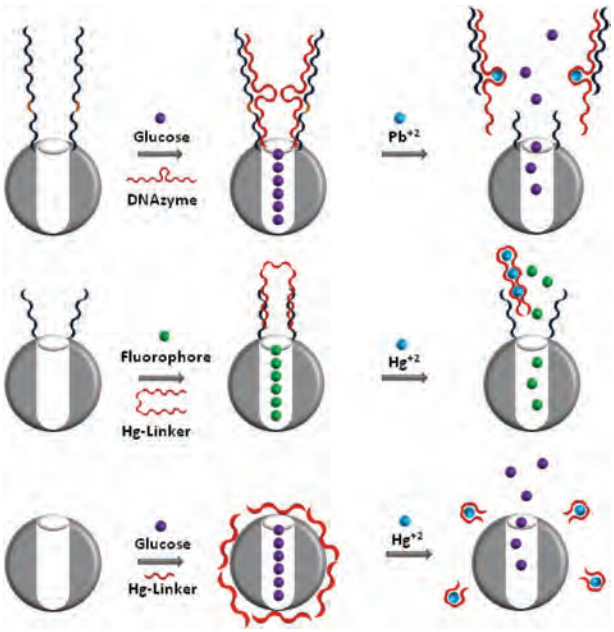

Fig. 10 Strategies developed for the DNA-based detection of heavy cations.

in a nanogate with improved capping efficiency,[195] a consequence of both double recognition sequences and the avidin–biotin bulkiness.

Apart from the already reviewed interesting DNAzyme based technology, there are other interesting strategies for the detection of pollutant heavy cations. For example, Hg^{+2} could be also detected employing DNA as it forms highly stable complexes bridging two thymine units in a linear complex.[196,197] This highly stable complex could be employed, if conveniently designed, to refold T-rich strands for detection purposes. A pioneering example by Tan and co-workers introduced the dsDNA capping strategy for the detection of mercury. In their model there were employed rhodamine loaded MSNs decorated with an anchor strand 5′-(GAA GAA CAA CAA AAA-NH_2)-3′ able to hybridize with the Hg^{+2}-linker 5′-(GTT GTT CTT CCT TTG TTT CCC CTT TCT TTG TTG TTC TTC)-3′ strand through a double pairing sequence (Fig. 10).[198] The sensing mechanism of this designed material was based on the employed linker strand, which was able to produce multiple T–Hg^{+2}–T bridges and to be displaced from the nanogate, allowing fluorophore release. Moreover, the device was tested against several common cations from which only Hg was able to produce effective dehybridization of the capping strand, demonstrating once again the potential of DNA for sensing applications. Another possible strategy for the detection of Hg, again based on a previous knowledge, was reported by Fang and co-workers; in their design the authors employed the thymine containing Hg^{+2}-sensitive 5′-(GAC ACA CTA GAC TAC TTT TCG)-3′ short oligonucleotide to wrap and seal the mesopores.[199] In this case, glucose was also employed as a detectable molecule (Fig. 10). In comparison with the other more complex nanosensor for cation detection, this last model pro-

vides a facile approach in which no expensive strands and fluorophores are required.

5.4 Sensors for the detection of enzymatic activity

Another interesting approach for the development of DNA–MSN based sensors is the detection of enzymatic activity, in particular, nucleases. These are enzymes widely present in intracellular environments and are responsible for degradation of extranuclear nucleic acids. This task is crucial as they maintain cell homeostasis regulating the elimination of messenger RNAs or viral genes, among other important tasks. The biological effect of nucleases is perfectly delimited while they are regulated, but their deregulation leads to severe problems. This is the case of telomerases, which play an important role in the development of cancer. For this reason it is important to have a set of tools for the intracellular measurement of enzymatic nuclease activity. With this idea in mind, Qu and co-workers developed a DNA–MSNs model able to detect the nuclease activity[42] (section 2.3). Their system, based on DNA grafting and complementary strand hybridization in the pore vicinity, was able to produce fluorophore release when deoxyribonuclease I was present. Although the purpose of this research was different, it set the principles for the development of nuclease sensing technology.

Although nuclease activity measurement could be of some interest for the development of sensors able to measure biological contamination, of greater interest is the development of nanodevices able to measure the presence of latent cancer diseases in a non-invasive way. For this purpose, Ju and co-workers developed a nanodevice able to the measure the presence of telomerase activity with a DNA–MSNs hybrid.[200] In their design the authors employed the telomerase substrate sequence 5′-[(CCC TAA)$_n$ AAT CCG TCG AGC AGA GTT]-3′ to coat electrostatically their NH_2-modified MSNs. The system was completed with a black hole quencher grafted into the internal pore walls; this produced fluorescence quenching unless telomerase-induced pore release of the loaded fluorescein occurred. The telomerase responsive device was tested against HeLa (breast) and BEL-7402 (liver) cancer cell lines obtaining in both examples fluorescence staining, while in the QSG-7701 (liver) healthy cells no fluorescence was obtained, thus validating the model for the detection of cancerous states in living cells. This telomerase sensor was later modified by Lu and co-workers to achieve detection with a commercially available glucometer. In this evolved model the authors employed again glucose-loaded cationic MSNs for the deposition of the cleavable 5′-[(CCC TAA)$_6$ AAT CCG TCG AGC AGA GTT]-3′ sequence.[201] Their use of glucose provided linear and direct measurements which allowed the authors to deepen the release studies, whose limit of detection was set at 80 HeLa cells per millilitre (Fig. 11).

The early detection of cancer together with the early and selective delivery of antiproliferative compounds to diseased cells is a strategy of interest for the development of future medicines. So, in a nice implementation of the telomerase sensor, Zong *et al.* reported the use of Dox loaded particles to treat the telomerase active HeLa cells.[202] Their design also included functional Ag@Au@MSNs core–shell particles which were employed for the surface-enhanced Raman spectroscopy (SERS) detection when taken up. Moreover, the possibilities of this system could go beyond a single therapeutic effect as there could also exert a combined chemo-photothermal effect.

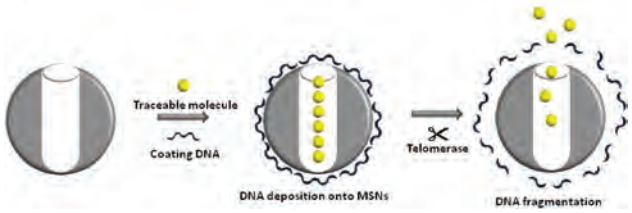

Fig. 11 DNA–MSN sensor based on the telomerase activity.

6. Conclusions

The present review covers the most prolific and relevant applications reported for the use of materials based on the joint use of nucleic acids and mesoporous silica nanoparticles. Special attention has been devoted to the development of novel nanodevices with potential application in either diagnostics or nanomedicine, because from a biomedical point of view, the incorporation of nucleic acids onto nanometre sized mesoporous silica has clearly advanced their biological behaviour. Some relevant research lines reviewed on this topic are the improvement of cellular recognition and vectorization, the possibility of modulating critical replication routes or the highly efficient and biocompatible nanogates sensitive to biogenic components. Moreover, the careful and rational design of nucleotides can fulfil several tasks, allowing the convergence of several relevant biological applications in a single device. Some of these visionary contributions show the path to follow in the development of multipurpose materials, in which mesoporous silica features its great modularity. Apart from the impressive biological features obtained for nucleotide–MSN hybrids, it is also remarkable that loading properties are barely interfered when nucleic acids are incorporated. The unaltered loading capacity, exemplified several times in the text, makes this particular combination of materials a highly interesting platform to develop future nanomedicines, diagnostic nanodevices or even their possible combinations. Of special interest is the development of hybrid materials for cancer therapy, mainly because of the significant advance they show in comparison with the classic chemotherapy. Hence, the use of nucleic acids could permit control over the destination of the therapeutic device and the disruption of crucial metabolic pathways while offering a responsive release of the drug reservoir which are mesoporous silica nanoparticles. Nevertheless, most of the models are still in a preliminary stage and much more effort should be devoted to the inorganic counterpart

and chemically modified nucleic acids to ensure full approval of their use in the clinic.

Acknowledgements

This work was supported by the European Research Council (Advanced Grant VERDI; ERC-2015-AdG, Proposal No. 694160) and the project MAT2015-64831-R.

Notes and references

1 S. S. Agasti, S. Rana, M.-H. Park, C. K. Kim, C.-C. You and V. M. Rotello, *Adv. Drug Delivery Rev.*, 2010, **62**, 316–328.
2 M. J. Sailor and J.-H. Park, *Adv. Mater.*, 2012, **24**, 3779–3802.
3 N. Ž. Knežević, E. Ruiz-Hernández, W. E. Hennink and M. Vallet-Regí, *RSC Adv.*, 2013, **3**, 9584–9593.
4 Y. Matsumura and H. Maeda, *Cancer Res.*, 1986, **46**, 6387–6392.
5 J. Fang, H. Nakamura and H. Maeda, *Adv. Drug Delivery Rev.*, 2011, **63**, 136–151.
6 H. Maeda, *Adv. Drug Delivery Rev.*, 2015, **91**, 3–6.
7 M. Vallet-Regí, F. Balas and D. Arcos, *Angew. Chem., Int. Ed.*, 2007, **46**, 7548–7558.
8 M. Martínez-Carmona, M. Colilla and M. Vallet-Regí, *Nanomaterials*, 2015, **5**, 1906–1937.
9 M. Vallet-Regi, A. Rámila, R. P. del Real and J. Pérez-Pariente, *Chem. Mater.*, 2001, **13**, 308–311.
10 A. Baeza, M. Colilla and M. Vallet-Regí, *Expert Opin. Drug Deliv.*, 2015, **12**, 319–337.
11 S. Giret, M. Wong Chi Man and C. Carcel, *Chem. – Eur. J.*, 2015, **21**, 13850–13865.
12 J. Lu, M. Liong, Z. Li, J. I. Zink and F. Tamanoi, *Small*, 2010, **6**, 1794–1805.
13 Q. He, Z. Zhang, F. Gao, Y. Li and J. Shi, *Small*, 2011, **7**, 271–280.
14 X. Huang, L. Li, T. Liu, N. Hao, H. Liu, D. Chen and F. Tang, *ACS Nano*, 2011, **5**, 5390–5399.
15 F. Tang, L. Li and D. Chen, *Adv. Mater.*, 2012, **24**, 1504–1534.
16 J. Liu, C. Detrembleur, S. Mornet, C. Jérôme and E. Duguet, *J. Mater. Chem. B*, 2015, **3**, 6117–6147.
17 E. Aznar, M. Oroval, L. Pascual, J. R. Murguía, R. Martínez-Máñez and F. Sancenón, *Chem. Rev.*, 2016, **116**, 561–718.
18 M. Vallet-Regí, M. Colilla and B. González, *Chem. Soc. Rev.*, 2011, **40**, 596–607.
19 M. Colilla, B. González and M. Vallet-Regí, *Biomater. Sci.*, 2013, **1**, 114–134.
20 A. Corma, *Chem. Rev.*, 1997, **97**, 2373–2420.
21 D. E. De Vos, M. Dams, B. F. Sels and P. A. Jacobs, *Chem. Rev.*, 2002, **102**, 3615–3640.
22 A. Taguchi and F. Schüth, *Microporous Mesoporous Mater.*, 2005, **77**, 1–45.
23 B. Korzeniowska, R. Nooney, D. Wencel and C. McDonagh, *Nanotechnology*, 2013, **24**, 442002.
24 F. Sancenón, L. Pascual, M. Oroval, E. Aznar and R. Martínez-Máñez, *ChemistryOpen*, 2015, **4**, 418–437.
25 D. Douroumis, I. Onyesom, M. Maniruzzaman and J. Mitchell, *Crit. Rev. Biotechnol.*, 2013, **33**, 229–245.
26 Z. Li, J. C. Barnes, A. Bosoy, J. F. Stoddart and J. I. Zink, *Chem. Soc. Rev.*, 2012, **41**, 2590–2605.
27 J. M. Rosenholm, J. Zhang, M. Linden and C. Sahlgren, *Nanomedicine*, 2016, **11**, 391–402.
28 E. Climent, R. Martínez-Máñez, F. Sancenón, M. D. Marcos, J. Soto, A. Maquieira and P. Amorós, *Angew. Chem., Int. Ed.*, 2010, **122**, 7439–7441.
29 Z. Liu, Y. Huang, F. Pu, J. Ren and X. Qu, *Chem. Commun.*, 2016, **52**, 3364–3367.
30 A. Schlossbauer, S. Warncke, P. M. E. Gramlich, J. Kecht, A. Manetto, T. Carell and T. Bein, *Angew. Chem., Int. Ed.*, 2010, **49**, 4734–4737.
31 E. Ruiz-Hernández, A. Baeza and M. Vallet-Regí, *ACS Nano*, 2011, **5**, 1259–1266.
32 L. A. Pray, *Nat. Educ.*, 2008, **1**, 100.
33 F. M. Martín-Saavedra, E. Ruíz-Hernández, A. Boré, D. Arcos, M. Vallet-Regí and N. Vilaboa, *Acta Biomater.*, 2010, **6**, 4522–4531.
34 C. S. S. R. Kumar and F. Mohammad, *Adv. Drug Delivery Rev.*, 2011, **63**, 789–808.
35 P. I. P. Soares, I. M. M. Ferreira, R. A. G. B. N. Igreja, C. M. M. Novo and J. P. M. R. Borges, *Recent Pat. Anticancer Drug Discov.*, 2012, **7**, 64–73.
36 S. Kossatz, J. Grandke, P. Couleaud, A. Latorre, A. Aires, K. Crosbie-Staunton, R. Ludwig, H. Dähring, V. Ettelt, A. Lazaro-Carrillo, M. Calero, M. Sader, J. Courty, Y. Volkov, A. Prina-Mello, A. Villanueva, Á. Somoza, A. L. Cortajarena, R. Miranda and I. Hilger, *Breast Cancer Res.*, 2015, **17**, 1–17.
37 L. Asín, M. R. Ibarra, A. Tres and G. F. Goya, *Pharm. Res.*, 2012, **29**, 1319–1327.
38 Y. Zhu and C. Tao, *RSC Adv.*, 2015, **5**, 22365–22372.
39 L. Chen, J. Di, C. Cao, Y. Zhao, Y. Ma, J. Luo, Y. Wen, W. Song, Y. Song and L. Jiang, *Chem. Commun.*, 2011, **47**, 2850–2852.
40 L. Pascual, I. Baroja, E. Aznar, F. Sancenón, M. D. Marcos, J. R. Murguía, P. Amorós, K. Rurack and R. Martínez-Máñez, *Chem. Commun.*, 2015, **51**, 1414–1416.
41 C. Chen, F. Pu, Z. Huang, Z. Liu, J. Ren and X. Qu, *Nucleic Acids Res.*, 2011, **39**, 1638–1644.
42 C. Chen, J. Geng, F. Pu, X. Yang, J. Ren and X. Qu, *Angew. Chem., Int. Ed.*, 2011, **50**, 882–886.
43 A. Schlossbauer, D. Schaffert, J. Kecht, E. Wagner and T. Bein, *J. Am. Chem. Soc.*, 2008, **130**, 12558–12559.
44 D. He, X. He, K. Wang, J. Cao and Y. Zhao, *Adv. Funct. Mater.*, 2012, **22**, 4704–4710.
45 H. Liu, Y. Xu, F. Li, Y. Yang, W. Wang, Y. Song and D. Liu, *Angew. Chem., Int. Ed.*, 2007, **46**, 2515–2517.
46 X. Yang, D. He, J. Cao, X. He, K. Wang and Z. Zou, *RSC Adv.*, 2015, **5**, 84553–84559.

47 C. Chen, L. Zhou, J. Geng, J. Ren and X. Qu, *Small*, 2013, **9**, 2793–2800.
48 Y. Lu and J. Liu, *Curr. Opin. Biotechnol.*, 2006, **17**, 580–588.
49 C. Teller, S. Shimron and I. Willner, *Anal. Chem.*, 2009, **81**, 9114–9119.
50 I. Willner, B. Shlyahovsky, M. Zayats and B. Willner, *Chem. Soc. Rev.*, 2008, **37**, 1153–1165.
51 M. Hollenstein, *Molecules*, 2015, **20**, 20777–20804.
52 J. Elbaz, S. Shimron and I. Willner, *Chem. Commun.*, 2010, **46**, 1209–1211.
53 J. Li, W. Zheng, A. H. Kwon and Y. Lu, *Nucleic Acids Res.*, 2000, **28**, 481–488.
54 F. Wang, J. Elbaz, C. Teller and I. Willner, *Angew. Chem., Int. Ed.*, 2011, **50**, 295–299.
55 Z. Zhang, D. Balogh, F. Wang and I. Willner, *J. Am. Chem. Soc.*, 2013, **135**, 1934–1940.
56 Z. Zhang, F. Wang, D. Balogh and I. Willner, *J. Mater. Chem. B*, 2014, **2**, 4449–4455.
57 J. Zhu, H. Huang, S. Dong, L. Ge and Y. Zhang, *Theranostics*, 2014, **4**, 931–944.
58 D. H. J. Bunka and P. G. Stockley, *Nat. Rev. Microbiol.*, 2006, **4**, 588–596.
59 E. Levy-Nissenbaum, A. F. Radovic-Moreno, A. Z. Wang, R. Langer and O. C. Farokhzad, *Trends Biotechnol.*, 2008, **26**, 442–449.
60 V. M. Tesmer, S. Lennarz, G. Mayer and J. J. G. Tesmer, *Structure*, 2012, **20**, 1300–1309.
61 C. Tuerk and L. Gold, *Science*, 1990, **249**, 505–510.
62 A. D. Ellington and J. W. Szostak, *Nature*, 1990, **346**, 818–822.
63 K. Sefah, D. Shangguan, X. Xiong, M. B. O'Donoghue and W. Tan, *Nat. Protoc.*, 2010, **5**, 1169–1185.
64 V. Bagalkot, O. C. Farokhzad, R. Langer and S. Jon, *Angew. Chem., Int. Ed.*, 2006, **45**, 8149–8152.
65 G. Zhu, G. Niu and X. Chen, *Bioconjugate Chem.*, 2015, **26**, 2186–2197.
66 J. Nicolas, S. Mura, D. Brambilla, N. Mackiewicz and P. Couvreur, *Chem. Soc. Rev.*, 2013, **42**, 1147–1235.
67 P. P. Deshpande, S. Biswas and V. P. Torchilin, *Nanomedicine*, 2013, **8**, 1509–1528.
68 L. Zhang, Y. Li and J. C. Yu, *J. Mater. Chem. B*, 2014, **2**, 452–470.
69 A. Samanta and I. L. Medintz, *Nanoscale*, 2016, **8**, 9037–9095.
70 J. R. Kanwar, K. Roy and R. K. Kanwar, *Crit. Rev. Biochem. Mol. Biol.*, 2011, **46**, 459–477.
71 J. E. Rosenberg, R. M. Bambury, E. M. Van Allen, H. A. Drabkin, P. N. Lara, A. L. Harzstark, N. Wagle, R. A. Figlin, G. W. Smith, L. A. Garraway, T. Choueiri, F. Erlandsson and D. A. Laber, *Invest. New Drugs*, 2014, **32**, 178–187.
72 E. M. Reyes-Reyes, F. R. Šalipur, M. Shams, M. K. Forsthoefel and P. J. Bates, *Mol. Oncol.*, 2015, **9**, 1392–1405.
73 L. Le Li, Q. Yin, J. Cheng and Y. Lu, *Adv. Healthcare Mater.*, 2012, **1**, 567–572.
74 X. Xie, F. Li, H. Zhang, Y. Lu, S. Lian, H. Lin, Y. Gao and L. Jia, *Eur. J. Pharm. Sci.*, 2016, **83**, 28–35.
75 L.-L. Li, M. Xie, J. Wang, X. Li, C. Wang, Q. Yuan, D.-W. Pang, Y. Lu and W. Tan, *Chem. Commun.*, 2013, **49**, 5823–5825.
76 C. Wang, L. Cheng and Z. Liu, *Theranostics*, 2013, **3**, 317–330.
77 B. E. Smith, P. B. Roder, X. Zhou and P. J. Pauzauskie, *Nanoscale*, 2015, **7**, 7115–7126.
78 X. Huang, P. K. Jain, I. H. El-Sayed and M. A. El-Sayed, *Lasers Med. Sci.*, 2008, **23**, 217–228.
79 L. Xu, L. Cheng, C. Wang, R. Peng and Z. Liu, *Polym. Chem.*, 2014, **5**, 1573–1580.
80 Y.-W. Chen, Y.-L. Su, S.-H. Hu and S.-Y. Chen, *Adv. Drug Delivery Rev.*, 2016, **105**, 190–204.
81 J. Wang and J. Qiu, *Cancer Res. Front.*, 2016, **2**, 67–84.
82 X. Yang, X. Liu, Z. Liu, F. Pu, J. Ren and X. Qu, *Adv. Mater.*, 2012, **24**, 2890–2895.
83 E. Ju, Z. Li, Z. Liu, J. Ren and X. Qu, *ACS Appl. Mater. Interfaces*, 2014, **6**, 4364–4370.
84 K. Wang, H. Yao, Y. Meng, Y. Wang, X. Yan and R. Huang, *Acta Biomater.*, 2015, **16**, 196–205.
85 Y. Tang, H. Hu, M. G. Zhang, J. Song, L. Nie, S. Wang, G. Niu, P. Huang, G. Lu and X. Chen, *Nanoscale*, 2015, **7**, 6304–6310.
86 Q. Liu, C. Jin, Y. Wang, X. Fang, X. Zhang, Z. Chen and W. Tan, *NPG Asia Mater.*, 2014, **6**, e95.
87 H. Sun and Y. Zu, *Small*, 2015, **11**, 2352–2364.
88 F. Jiang, B. Liu, J. Lu, F. Li, D. Li, C. Liang, L. Dang, J. Liu, B. He, S. A. Badshah, C. Lu, X. He, B. Guo, X. B. Zhang, W. Tan, A. Lu and G. Zhang, *Int. J. Mol. Sci.*, 2015, **16**, 23784–23822.
89 V. C. Ozalp, F. Eyidogan and H. A. Oktem, *Pharmaceuticals*, 2011, **4**, 1137–1157.
90 C. Zhu, C. Lu, X. Song, H. Yang and X.-R. Wang, *J. Am. Chem. Soc.*, 2011, **133**, 1278–1281.
91 X. He, Y. Zhao, D. He, K. Wang, F. Xu and J. Tang, *Langmuir*, 2012, **28**, 12909–12915.
92 F. J. Hernandez, L. I. Hernandez, A. Pinto, T. Schafer and V. C. Ozalp, *Chem. Commun.*, 2013, **49**, 1285–1287.
93 Y. Zhang, Z. Hou, Y. Ge, K. Deng, B. Liu, X. Li, Q. Li, Z. Cheng, P. Ma, C. Li and J. Lin, *ACS Appl. Mater. Interfaces*, 2015, **7**, 20696–20706.
94 P. Zhang, F. Cheng, R. Zhou, J. Cao, J. Li, C. Burda, Q. Min and J. J. Zhu, *Angew. Chem., Int. Ed.*, 2014, **53**, 2371–2375.
95 A. M. Krichevsky and G. Gabriely, *J. Cell. Mol. Med.*, 2008, **13**, 39–53.
96 R. Kanasty, J. R. Dorkin, A. Vegas and D. Anderson, *Nat. Mater.*, 2013, **12**, 967–977.
97 Q. Yin, J. Shen, Z. Zhang, H. Yu and Y. Li, *Adv. Drug Delivery Rev.*, 2013, **65**, 1699–1715.
98 F. Geinguenaud, E. Guenin, Y. Lalatonne and L. Motte, *ACS Chem. Biol.*, 2016, **11**, 1180–1191.
99 N. Ž. Knežević and J.-O. Durand, *Nanoscale*, 2015, **7**, 2199–2209.

100 I. I. Slowing, B. G. Trewyn and V. S.-Y. Lin, *J. Am. Chem. Soc.*, 2007, **129**, 8845–8849.
101 M. Fujiwara, F. Yamamoto, K. Okamoto, K. Shiokawa and R. Nomura, *Anal. Chem.*, 2005, **77**, 8138–8145.
102 F. Gao, P. Botella, A. Corma, J. Blesa and L. Dong, *J. Phys. Chem. B*, 2009, **113**, 1796–1804.
103 F. Qin, Y. Zhou, J. Shi and Y. Zhang, *J. Biomed. Mater. Res. A*, 2009, **90**, 333–338.
104 J. L. Steinbacher and C. C. Landry, *Langmuir*, 2014, **30**, 4396–4405.
105 X. Li, J. Zhang and H. Gu, *Langmuir*, 2011, **27**, 6099–6106.
106 X. Li, Y. Chen, M. Wang, Y. Ma, W. Xia and H. Gu, *Biomaterials*, 2013, **34**, 1391–1401.
107 M.-H. Kim, H. Na, Y. Kim, S. Ryoo, H. S. Cho, K. E. Lee, H. Jeon, R. Ryoo and D.-H. Min, *ACS Nano*, 2011, **5**, 3568–3576.
108 H. K. Na, M. H. Kim, K. Park, S. R. Ryoo, K. E. Lee, H. Jeon, R. Ryoo, C. Hyeon and D. H. Min, *Small*, 2012, **8**, 1752–1761.
109 S. B. Hartono, W. Gu, F. Kleitz, J. Liu, L. He, A. P. J. Middelberg, C. Yu, G. Q. Lu and S. Z. Qiao, *ACS Nano*, 2012, **6**, 2104–2117.
110 D. Niu, Z. Liu, Y. Li, X. Luo, J. Zhang, J. Gong and J. Shi, *Adv. Mater.*, 2014, **26**, 4947–4953.
111 X. Huang, Z. Tao, J. C. Praskavich, A. Goswami, J. F. Al-Sharab, T. Minko, V. Polshettiwar and T. Asefa, *Langmuir*, 2014, **30**, 10886–10898.
112 A. K. Meka, Y. Niu, S. Karmakar, S. B. Hartono, J. Zhang, C. X. C. Lin, H. Zhang, A. Whittaker, K. Jack, M. Yu and C. Yu, *ChemNanoMat*, 2016, **2**, 220–225.
113 J. Zhang, M. Niemelä, J. Westermarck and J. M. Rosenholm, *Dalton Trans.*, 2014, **43**, 4115–4126.
114 K. Möller, K. Müller, H. Engelke, C. Bräuchle, E. Wagner and T. Bein, *Nanoscale*, 2016, **8**, 4007–4019.
115 C. E. Ashley, E. C. Carnes, K. E. Epler, D. P. Padilla, G. K. Phillips, R. E. Castillo, D. C. Wilkinson, B. S. Wilkinson, C. A. Burgard, R. M. Kalinich, J. L. Townson, B. Chackerian, C. L. Willman, D. S. Peabody, W. Wharton and C. J. Brinker, *ACS Nano*, 2012, **6**, 2174–2188.
116 L. Li, J. Hou, X. Liu, Y. Guo, Y. Wu, L. Zhang and Z. Yang, *Biomaterials*, 2014, **35**, 3840–3850.
117 K. A. Whitehead, R. Langer and D. G. Anderson, *Nat. Rev. Drug Discovery*, 2009, **8**, 129–138.
118 Y.-K. Oh and T. G. Park, *Adv. Drug Delivery Rev.*, 2009, **61**, 850–862.
119 D. J. Gary, N. Puri and Y.-Y. Won, *J. Controlled Release*, 2007, **121**, 64–73.
120 W. J. Kim and S. W. Kim, *Pharm. Res.*, 2009, **26**, 657–666.
121 R. S. Shukla, B. Qin and K. Cheng, *Mol. Pharm.*, 2014, **11**, 3395–3408.
122 J. Yang, Q. Zhang, H. Chang and Y. Cheng, *Chem. Rev.*, 2015, **115**, 5274–5300.
123 Y. Wang, L. Miao, A. Satterlee and L. Huang, *Adv. Drug Delivery Rev.*, 2015, **87**, 68–80.
124 Y. Ding, Z. Jiang, K. Saha, C. S. Kim, S. T. Kim, R. F. Landis and V. M. Rotello, *Mol. Ther.*, 2014, **22**, 1075–1083.
125 B. Yu, X. Zhao, L. J. Lee and R. J. Lee, *AAPS J.*, 2009, **11**, 195–203.
126 P. Kesharwani, V. Gajbhiye and N. K. Jain, *Biomaterials*, 2012, **33**, 7138–7150.
127 A. Akinc, M. Thomas, A. M. Klibanov and R. Langer, *J. Gene Med.*, 2005, **7**, 657–663.
128 A. K. Varkouhi, M. Scholte, G. Storm and H. J. Haisma, *J. Controlled Release*, 2011, **151**, 220–228.
129 J. Kim, J. Kim, C. Jeong and W. J. Kim, *Adv. Drug Delivery Rev.*, 2016, **98**, 99–112.
130 R. R. Castillo, M. Colilla and M. Vallet-Regí, *Expert Opin. Drug Deliv.*, 2017, **14**, 229–243.
131 D. R. Radu, C. Y. Lai, K. Jeftinija, E. W. Rowe, S. Jeftinija and V. S. Y. Lin, *J. Am. Chem. Soc.*, 2004, **126**, 13216–13217.
132 F. Torney, B. G. Trewyn, V. S.-Y. Lin and K. Wang, *Nat. Nanotechnol.*, 2007, **2**, 295–300.
133 S. Martin-Ortigosa, J. S. Valenstein, V. S. Y. Lin, B. G. Trewyn and K. Wang, *Adv. Funct. Mater.*, 2012, **22**, 3576–3582.
134 S. Martin-Ortigosa, D. J. Peterson, J. S. Valenstein, V. S.-Y. Lin, B. G. Trewyn, L. A. Lyznik and K. Wang, *Plant Physiol.*, 2014, **164**, 537–547.
135 R. A. Gemeinhart, D. Luo and W. M. Saltzman, *Biotechnol. Prog.*, 2005, **21**, 532–537.
136 S. M. Solberg and C. C. Landry, *J. Phys. Chem. B*, 2006, **110**, 15261–15268.
137 I. I. Slowing, J. L. Vivero-Escoto, C.-W. Wu and V. S. Y. Lin, *Adv. Drug Delivery Rev.*, 2008, **60**, 1278–1288.
138 Y. Jiang, S. Huo, J. Hardie, X. Liang and V. M. Rotello, *Expert Opin. Drug Deliv.*, 2016, **13**, 547–559.
139 I. Y. Park, I. Y. Kim, M. K. Yoo, Y. J. Choi, M. H. Cho and C. S. Cho, *Int. J. Pharm.*, 2008, **359**, 280–287.
140 T. Xia, M. Kovochich, M. Liong, H. Meng, S. Kabehie, S. George, J. I. Zink and A. E. Nel, *ACS Nano*, 2009, **3**, 3273–3286.
141 X. Wang, S. Masse, G. Laurent, C. Hélary and T. Coradin, *Langmuir*, 2015, **31**, 11078–11085.
142 Y. Kapilov-Buchman, E. Lellouche, S. Michaeli and J.-P. Lellouche, *Bioconjugate Chem.*, 2015, **26**, 880–889.
143 M. Yu, Y. Niu, Y. Yang, S. B. Hartono, J. Yang, X. Huang, P. Thorn and C. Yu, *ACS Appl. Mater. Interfaces*, 2014, **6**, 15626–15631.
144 W. Ngamcherdtrakul, J. Morry, S. Gu, D. J. Castro, S. M. Goodyear, T. Sangvanich, M. M. Reda, R. Lee, S. A. Mihelic, B. L. Beckman, Z. Hu, J. W. Gray and W. Yantasee, *Adv. Funct. Mater.*, 2015, **25**, 2646–2659.
145 M. Wu, Q. Meng, Y. Chen, Y. Du, L. Zhang, Y. Li, L. Zhang and J. Shi, *Adv. Mater.*, 2015, **27**, 215–222.
146 N. D'Onofrio, M. Caraglia, A. Grimaldi, R. Marfella, L. Servillo, G. Paolisso and M. L. Balestrieri, *Biochim. Biophys. Acta*, 2014, **1846**, 1–12.

147 J. Lu, H.-H. Shen, Z. Wu, B. Wang, D. Zhao and L. He, *J. Mater. Chem. B*, 2015, **3**, 7653–7657.
148 Á. Martínez, E. Fuentes-Paniagua, A. Baeza, J. Sánchez-Nieves, M. Cicuéndez, R. Gómez, F. J. de la Mata, B. González and M. Vallet-Regí, *Chem. – Eur. J.*, 2015, **21**, 15651–15666.
149 L. Liu, Z. Guo, Z. Huang, J. Zhuang and W. Yang, *Sci. Rep.*, 2016, **6**, 22029.
150 M. Creixell and N. A. Peppas, *Nano Today*, 2012, **7**, 367–379.
151 P. Y. Teo, W. Cheng, J. L. Hedrick and Y. Y. Yang, *Adv. Drug Delivery Rev.*, 2016, **98**, 41–63.
152 M. M. Gottesman, T. Fojo and S. E. Bates, *Nat. Rev. Cancer*, 2002, **2**, 48–58.
153 R. J. Kathawala, P. Gupta, C. R. Ashby Jr. and Z.-S. Chen, *Drug Resist. Updat.*, 2015, **18**, 1–17.
154 R. J. Youle and A. Strasser, *Nat. Rev. Mol. Cell Biol.*, 2008, **9**, 47–59.
155 P. E. Czabotar, G. Lessene, A. Strasser and J. M. Adams, *Nat. Rev. Mol. Cell Biol.*, 2013, **15**, 49–63.
156 X. Wang, M. Chen, J. Zhou and X. Zhang, *Int. J. Oncol.*, 2014, **45**, 18–30.
157 A. M. Chen, M. Zhang, D. Wei, D. Stueber, O. Taratula, T. Minko and H. He, *Small*, 2009, **5**, 2673–2677.
158 X. Ma, Y. Zhao, K. W. Ng and Y. Zhao, *Chem. – Eur. J.*, 2013, **19**, 15593–15603.
159 H. Meng, M. Liong, T. Xia, Z. Li, Z. Ji, J. I. Zink and A. E. Nel, *ACS Nano*, 2010, **4**, 4539–4550.
160 H. Meng, W. X. Mai, H. Zhang, M. Xue, T. Xia, S. Lin, X. Wang and Y. Zhao, *ACS Nano*, 2013, **7**, 994–1005.
161 M. Wu, Q. Meng, Y. Chen, L. Zhang, M. Li, X. Cai, Y. Li, P. Yu, L. Zhang and J. Shi, *Adv. Mater.*, 2016, **28**, 1963–1969.
162 S. R. Bhattarai, E. Muthuswamy, A. Wani, M. Brichacek, A. L. Castañeda, S. L. Brock and D. Oupicky, *Pharm. Res.*, 2010, **27**, 2556–2568.
163 S. B. Hartono, N. T. Phuoc, M. Yu, Z. Jia, M. J. Monteiro, S. Qiao and C. Yu, *J. Mater. Chem. B*, 2014, **2**, 718–726.
164 A. Bertucci, E. A. Prasetyanto, D. Septiadi, A. Manicardi, E. Brognara, R. Gambari, R. Corradini and L. De Cola, *Small*, 2015, **11**, 5687–5695.
165 L. Han, C. Tang and C. Yin, *Biomaterials*, 2015, **60**, 42–52.
166 H. Gu, Y. Chen, X. Wang, T. Liu, D. S. Zhang, Y. Wang and W. Di, *Int. J. Nanomedicine*, 2015, **10**, 2579–2594.
167 Y. T. Chang, P. Y. Liao, H. S. Sheu, Y. J. Tseng, F. Y. Cheng and C. S. Yeh, *Adv. Mater.*, 2012, **24**, 3309–3314.
168 K. Wang, Z. Tang, C. J. Yang, Y. Kim, X. Fang, W. Li, Y. Wu, C. D. Medley, Z. Cao, J. Li, P. Colon, H. Lin and W. Tan, *Angew. Chem., Int. Ed.*, 2009, **48**, 856–870.
169 D. S. Seferos, D. A. Giljohann, H. D. Hill, A. E. Prigodich and C. A. Mirkin, *J. Am. Chem. Soc.*, 2007, **129**, 15477–15479.
170 S. Song, Z. Liang, J. Zhang, L. Wang, G. Li and C. Fan, *Angew. Chem., Int. Ed.*, 2009, **48**, 8670–8674.
171 J. Conde, J. Rosa, J. M. de la Fuente and P. V. Baptista, *Biomaterials*, 2013, **34**, 2516–2523.
172 B. Deng, Y. Lin, C. Wang, F. Li, Z. Wang, H. Zhang, X.-F. Li and X. C. Le, *Anal. Chim. Acta*, 2014, **837**, 1–15.
173 C. Feng, S. Dai and L. Wang, *Biosens. Bioelectron.*, 2014, **59**, 64–74.
174 Z. Mei, H. Chu, W. Chen, F. Xue, J. Liu, H. Xu, R. Zhang and L. Zheng, *Biosens. Bioelectron.*, 2013, **39**, 26–30.
175 M. Hasanzadeh, N. Shadjou, M. de la Guardia, M. Eskandani and P. Sheikhzadeh, *TrAC, Trends Anal. Chem.*, 2012, **33**, 117–129.
176 M. Etienne, L. Zhang, N. Vilà and A. Walcarius, *Electroanalysis*, 2015, **27**, 2028–2054.
177 S. H. Joo, J. Y. Park, C.-K. Tsung, Y. Yamada, P. Yang and G. A. Somorjai, *Nat. Mater.*, 2009, **8**, 126–131.
178 H. Li, J. He, Y. Zhao, D. Wu, Y. Cai, Q. Wei and M. Yang, *Electrochim. Acta*, 2011, **56**, 2960–2965.
179 K. Ren, J. Wu, Y. Zhang, F. Yan and H. Ju, *Anal. Chem.*, 2014, **86**, 7494–7499.
180 J. Zhang, Y. Chai, R. Yuan, Y. Yuan, L. Bai and S. Xie, *Analyst*, 2013, **138**, 6938–6945.
181 E. Torres-Chavolla and E. C. Alocilja, *Biosens. Bioelectron.*, 2009, **24**, 3175–3182.
182 H. Li, Y. Mu, S. Qian, J. Lu, Y. Wan, G. Fu and S. Liu, *Analyst*, 2015, **140**, 567–573.
183 J. Wang, X.-L. Li, J.-D. Zhang, N. Hao, J.-J. Xu and H.-Y. Chen, *Chem. Commun.*, 2015, **51**, 11673–11676.
184 M. Montalti, L. Prodi, E. Rampazzo and N. Zaccheroni, *Chem. Soc. Rev.*, 2014, **43**, 4243–4268.
185 X. Wang, P. Song, L. Peng, A. Tong and Y. Xiang, *ACS Appl. Mater. Interfaces*, 2016, **8**, 609–616.
186 Y. Xiong, C. Deng, X. Zhang and P. Yang, *ACS Appl. Mater. Interfaces*, 2015, **7**, 8451–8456.
187 Y. Dai, A. Zhang, J. You, J. Li, H. Xu and K. Xu, *RSC Adv.*, 2015, **5**, 77204–77210.
188 J. Tan, N. Yang, Z. Hu, J. Su, J. Zhong, Y. Yang, Y. Yu, J. Zhu, D. Xue, Y. Huang, Z. Lai, Y. Huang, X. Lu and Y. Zhao, *Nanoscale Res. Lett.*, 2016, **11**, 298.
189 H. Jo, J. Her and C. Ban, *Biosens. Bioelectron.*, 2015, **71**, 129–136.
190 L. Cai, Z. Z. Chen, X. M. Dong, H. W. Tang and D. W. Pang, *Biosens. Bioelectron.*, 2011, **29**, 46–52.
191 L. Lu, Y. Qian, L. Wang, K. Ma and Y. Zhang, *ACS Appl. Mater. Interfaces*, 2014, **6**, 1944–1950.
192 S. Wu, H. Zhang, Z. Shi, N. Duan, C. Fang, S. Dai and Z. Wang, *Food Control*, 2015, **50**, 597–604.
193 F. Pu, Z. Liu, J. Ren and X. Qu, *Chem. Commun.*, 2013, **49**, 2305–2307.
194 L. B. Fu, J. Y. Zhuang, W. Q. Lai, X. H. Que, M. H. Lu and D. P. Tang, *J. Mater. Chem. B*, 2013, **1**, 6123–6128.
195 W. Song, J. Li, Q. Li, W. Ding and X. Yang, *Anal. Biochem.*, 2015, **471**, 17–22.
196 S. Katz, *Nature*, 1962, **194**, 569–569.
197 Y. Miyake, H. Togashi, M. Tashiro, H. Yamaguchi, S. Oda, M. Kudo, Y. Tanaka, Y. Kondo, R. Sawa, T. Fujimoto,

T. Machinami and A. Ono, *J. Am. Chem. Soc.*, 2006, **128**, 2172–2173.
198 Y. Zhang, Q. Yuan, T. Chen, X. Zhang, Y. Chen and W. Tan, *Anal. Chem.*, 2012, **84**, 1956–1962.
199 X. Liang, L. Wang, D. Wang, L. Zeng and Z. Fang, *Chem. Commun.*, 2016, **52**, 2192–2194.
200 R. Qian, L. Ding and H. Ju, *J. Am. Chem. Soc.*, 2013, **135**, 13282–13285.
201 Y. Wang, M. Lu, J. Zhu and S. Tian, *J. Mater. Chem. B*, 2014, **2**, 5847–5853.
202 S. Zong, Z. Wang, H. Chen, D. Zhu, P. Chen and Y. Cui, *IEEE Trans. Nanobioscience*, 2014, **13**, 55–60.